Defence Research and Development Canada
Recherche et développement pour la défense Canada

DEFENCE R&D DÉFENSE

Surveillance Through Concrete Walls

Sylvain Gauthier, Eric Hung and Walid Chamma

Defence R&D Canada – Ottawa
TECHNICAL MEMORANDUM
DRDC Ottawa TM 2003-233
December 2003

Canada

SURVEILLANCE THROUGH CONCRETE WALLS

Sylvain Gauthier
Eric Hung
Walid Chamma

Defence R&D Canada – Ottawa

Technical Memorandum

DRDC Ottawa TM 2003-233

December 2003

© Her Majesty the Queen as represented by the Minister of National Defence, 2003

© Sa majesté la reine, représentée par le ministre de la Défense nationale, 2003

Abstract

This report studies the capability of ultra wideband short-pulse (UWB SP) radar to provide through concrete walls surveillance including multistatic radar surveillance. Multistatic radar configurations are of interest since they can be used to do covert surveillance.

A full wave electromagnetic simulator is used to generate high fidelity through wall radar data. These raw radar data are transformed into radar images using a generation image algorithm that is described in detail in this report. The delay of the electromagnetic wave due to concrete walls when included into the imaging algorithm considerably improves the radar images. The impact of various radar parameters and signal processing techniques on radar images are examined in detail. The goal is to optimize the development of a potential radar testbed for through-wall imaging applications.

Radar images obtained using the image generation algorithm show that UWB SP radar can track targets moving inside a concrete room. The decrease in signal velocity within concrete walls has three effects on through-the-wall-imaging. It defocuses target images and displaces targets from their true positions. False targets can also be present in the radar images.

The radar images are considerably improved by including the time of flight difference due to concrete walls into the image generation algorithm. Radar images of stationary objects, or the room layout, obtained using the image generation algorithm show that UWB SP radar can provide static mapping of the concrete room layout. Radar images obtained using different multistatic radar configurations show that multistatic imaging works as long as targets are not located in the direct coupling region.

Résumé

Ce rapport étudie la capacité des radars à courte impulsion et très large bande de fréquence (UWB SP) pour effectuer de la surveillance à travers des murs de ciments. Cette étude examine aussi l'utilisation de radar multistatiques. Les radars multistatiques sont d'intérêt puisqu'ils peuvent utiliser pour de la surveillance passive.

Un logiciel de simulation d'onde électromagnétique est utilisé pour générer des données simulées de hautes fidélités. Les données simulées sont transformées en images radars par un algorithme de génération d'images lequel est décrit dans ce rapport. Les images radars sont de meilleures qualités quand on y inclut le délai de l'onde électromagnétique due au mur de ciments. L'impact de différent paramètre radars ou de traitement de signaux sont examinée en détails. Le but est d'optimisé le développent d'un système radar pour des applications d'imageries à travers les murs.

Les radars images obtenues en utilisant l'algorithme de génération d'images montrent que les radars UWB SP peuvent traquer des cibles se déplaçant à l'intérieur d'un édifice en ciment. Les murs de ciments ont trois impacts sur les images radars. Les images des cibles sont de-focussées et déplacées par rapport à leurs vraies positions. Des fausses cibles peuvent aussi être présentes sur les images radars. Les images radars des objets stationnaires montrent que les radars UWB SP peuvent fournir des cartes de la disposition de la pièce incluant la position des cibles. Les images radars obtenus en utilisant des configurations multistatiques montrent que les imageries multistatiques fonctionnent bien aussi longtemps que les cibles ne sont pas placées entre l'antenne qui transmet et l'antenne qui reçoit. Plus précisément quand les cibles ne sont pas dans la région de couplage directe ou que le signal direct arrive avant le signal indirect, i.e., between the transmitting and receiving antennas.

Executive summary

This report studies the feasibility of using ultra wideband short-pulse (UWB SP) radar to provide surveillance through concrete walls. Buildings with concrete or brick walls are very common throughout the world and are the most likely type of building to be encountered by the CF when performing military operations in urban terrain.

A full wave electromagnetic simulator is used to generate high fidelity through wall radar data. The raw radar data are transformed into radar images using a generation image algorithm.

The velocity of the electromagnetic wave inside a concrete wall is reduced compared to free space. This effect defocuses target images, displaces them from their true positions and can produce false targets on the radar images. These can be fixed by including the time of flight difference due to the concrete walls into the image generation algorithm.

Radar images of moving targets are examined in detail for various conditions. Images can be improved by first subtracting fixed clutter from the received signals. These improved images show that UWB SP radar can track targets moving inside concrete room.

Radar images of stationary objects have also been produced and studied in detail. Once again, the results show that UWB SP radar can provide static mapping of the concrete room layout including the stationary objects.

The last section studies the capability of multistatic UWB SP radar to provide through wall surveillance. Radar images for various multistatic radar configurations are produced for this purpose. The results show that multistatic imaging works well, as long as the targets are not located in the direct coupling region, i.e., between the transmitting and receiving antennas.

Sylvain Gauthier, Eric Hung, Walid Chamma, 2003, Surveillance Through Concrete Walls, DRDC Ottawa TM 2003-233, Defence R&D Canada - Ottawa.

Sommaire

Ce rapport étudie la capacité des radars à courte impulsion et très large bande de fréquence (UWB SP) pour effectuer de la surveillance à travers des murs de ciments.
Les édifices avec des murs de ciments ou en briques sont très communs a travers le monde et sont les édifices les plus probables d'être rencontrer par le forces canadiennes opérant en milieu urbain.

Un logiciel de simulation d'onde électromagnétique est utilisé pour générer des données simulées de hautes fidélités. Les données simulées sont transformées en images radars par un algorithme de génération d'images lequel est décrit dans ce rapport. La vitesse des ondes électromagnétiques est réduite à l'intérieur des murs de ciments. Ceci a pour effet de dé-focussé les images radars, de déplacer les cibles par rapport à leurs vraies positions et peut produire de fausses cibles. Ces effets peuvent être corrigés en incluant le délai de l'onde électromagnétique due au mur de ciments dans l'algorithme de génération d'images.

Les radars images obtenues en utilisant l'algorithme de génération d'images montrent que les radars UWB SP peuvent traquer des cibles se déplaçant à l'intérieur d'un édifice en ciment. Les images radars des objets stationnaires montrent que les radars UWB SP peuvent fournir des cartes de la disposition de la pièce incluant la position des cibles.

Cette étude examine aussi l'utilisation de radar multistatiques. Les radars multistatiques sont d'intérêt puisqu'ils peuvent utiliser pour de la surveillance passive. Les images radars obtenus en utilisant des configurations multistatiques montrent que les imageries multistatiques fonctionnent bien aussi longtemps que les cibles ne sont pas placées entre l'antenne qui transmet et l'antenne qui reçoit. Plus précisément quand les cibles ne sont pas dans la région de couplage directe ou que le signal direct arrive avant le signal indirect.

Sylvain Gauthier, Eric Hung, Walid Chamma, 2003, Surveillance Through Concrete Walls, DRDC Ottawa TM 2003-233, R & D pour la défense Canada - Ottawa

Table of contents

List of figures

List of tables

1. Introduction

DRDC Ottawa has been studying the capability of ultra wideband short-pulse (UWB SP) radar to provide through the wall surveillance since 2001 [1-12]. References [3] and [4] have clearly demonstrated the feasibility of tracking a target moving behind a wooden wall using UWB SP radar.

This report studies the feasibility of using UWB SP radar to provide through concrete wall surveillance. Buildings with concrete or brick walls are very common throughout the world and are the most likely type of building to be encountered by the CF when performing military operations in urban terrain [14]. This report completes the through concrete wall surveillance study initiated in [10] and [13].

In [12], Comlab Inc demonstrated that a radar can produce radar images of targets moving behind a wall of concrete blocks. They used their experimental UWB SP radar operating at a center frequency of 10GHz for this purpose. In this report, the targets images were defocused and also multiple peaks were associated with a target. The difference is due to concrete blocks having cavities that produce more internal reflection.

Simulated data of an UWB SP radar in front of a concrete room have been generated for the through–concrete-wall study. Section 2 describes the modeling of the UWB SP radar and the concrete room, including two moving targets.

Section 3 describes the image generation algorithm used to process the received signals into radar images. This algorithm is based on the back projection technique that consists of adding each receiver range return on a spatial grid [3]. Signal propagation in the concrete wall will alter the total return time of the signal, which will defocus the radar images. This section will describe how to calculate this time difference and how to compensate for it in the back projection algorithm.

In Section 4, radar images of moving targets were generated by subtracting fixed clutter from the received signals, or by use of moving target indicator (MTI) procedures. The section examines radar images generated with and without compensation for the timing effects caused by signals propagating through the concrete walls. Section 5 examines radar images from returns from stationary objects.

Section 6 examines the impact of various radar and signal processing parameters on the through concrete wall images in order to optimize the parameters of UWB SP radar. Parameters examined include: sampling rate, pixel sizes, receiver antenna aperture size and element spacing.

Section 7 studies the capability of multi-static UWB SP radar to provide through wall surveillance. A UWB SP transmitter on a UAV could be used to illuminate a building while soldiers conduct covert through-wall surveillance on the ground.

2. Electromagnetic modeling and simulation

Simulated data of an UWB SP radar in front of a concrete room have been generated for the through concrete wall study. Section 2.1 describes the modeling of the UWB SP radar, the concrete room, and two moving targets. Sub-section 2.2 shows that UWB SP signals can propagate through concrete walls and illuminate targets inside. Sub-section 2.3 examines the received signals with and without walls blocking the target. These received echoes will be used to produce radar images of the illuminated scenes.

2.1 Electromagnetic modeling

The electromagnetic software used for this project is based on the finite-difference time-domain (FDTD) method, which is a direct solution of the time-dependent Maxwell's curl equations using the finite-difference technique. It is analogous to the finite-difference solution of fluid flow problems encountered in computational aerodynamics, where a numerical model is based on a direct solution of the corresponding partial differential equations. In FDTD the propagation of an EM wave in a volume of space containing a dielectric or a conducting structure (or a combination of both) is modeled. By time stepping, the incident wave transmitted from an antenna is tracked as it first propagates to the structure and then interacts with the latter through current excitation, scattering, multiple scattering, penetration and diffraction.

Figure 1 and Figure 2 show the dimensions of the concrete room and the two cubic conductors inside the room. The external dimensions of the room are 2.47 m wide, 3.7 m long and 2.75 m high. The room floor, ceiling and walls are all concrete. The conductivity and relative permittivity of the concrete walls have been set to 0.05 S/m and 7 respectively. By definition, the relative permittivity has no units. The UWB SP radar is modeled as a single transmitting antenna consisting of a 9 cm vertical dipole located 1 m above ground and 11 cm in front of the concrete room. The electromagnetic field is recorded every 2 cm around the room to simulate receive signals. This gives us the flexibility to study the receiving array of different size, antenna spacing and at various positions. The numbering scheme use in Figure 1 and how it relates to the receiver antenna position is described in Annex B. The dimensions of the two metallic cubes are 10x10x10 cm^3 and 30x30x30 cm^3. Thirty different positions have been modeled for the two boxes to simulate targets in motion (See Annex A). Transmitting an UWB SP signal and recording the reflected echoes for each box position simulate motion. A 0.5 nanosecond pulse, shown in Figure 3, excites the vertical transmitting dipole antenna. The radiated electromagnetic field is also shown in the figure.

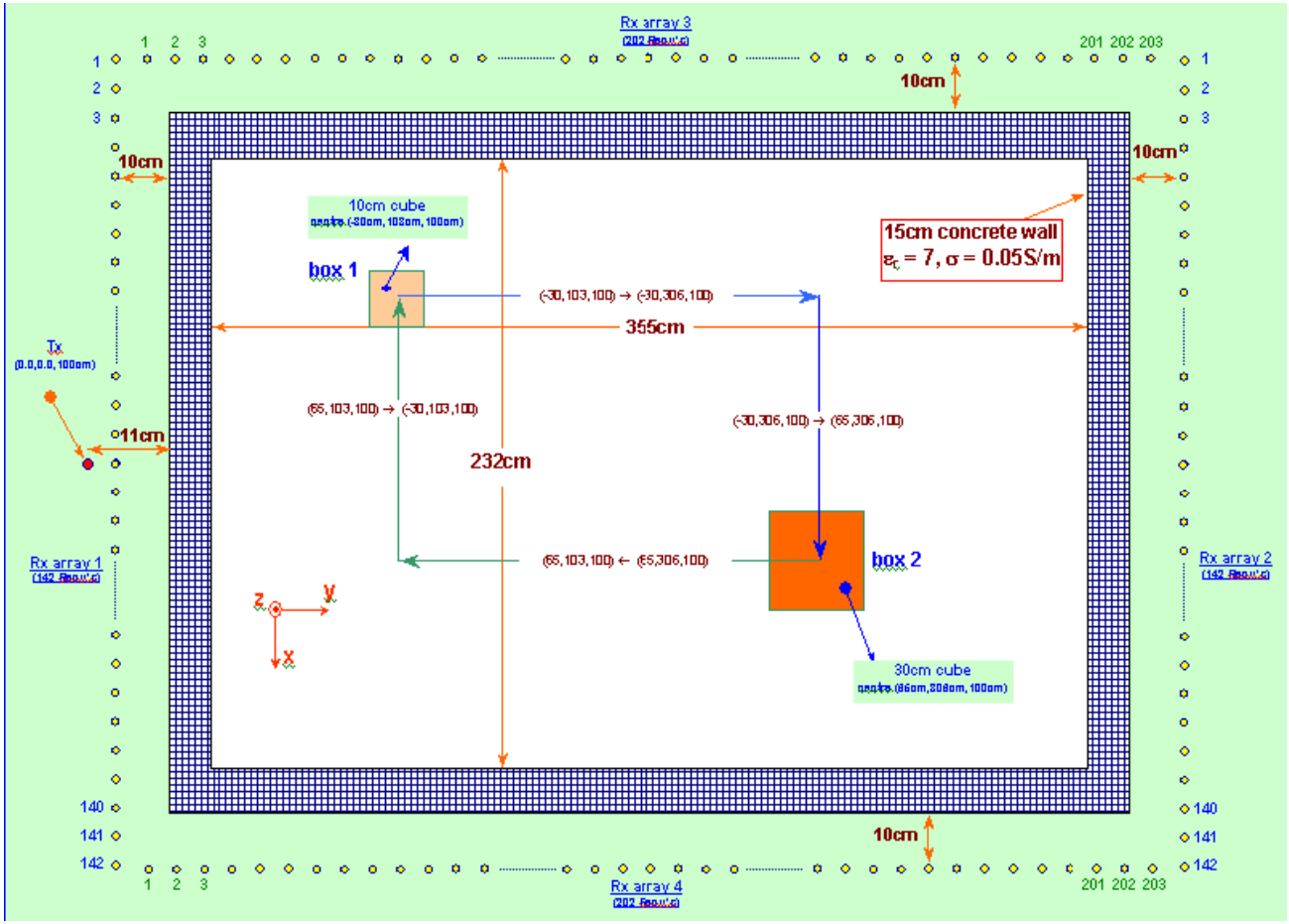

Figure 1. Top view of simulated concrete room scenario

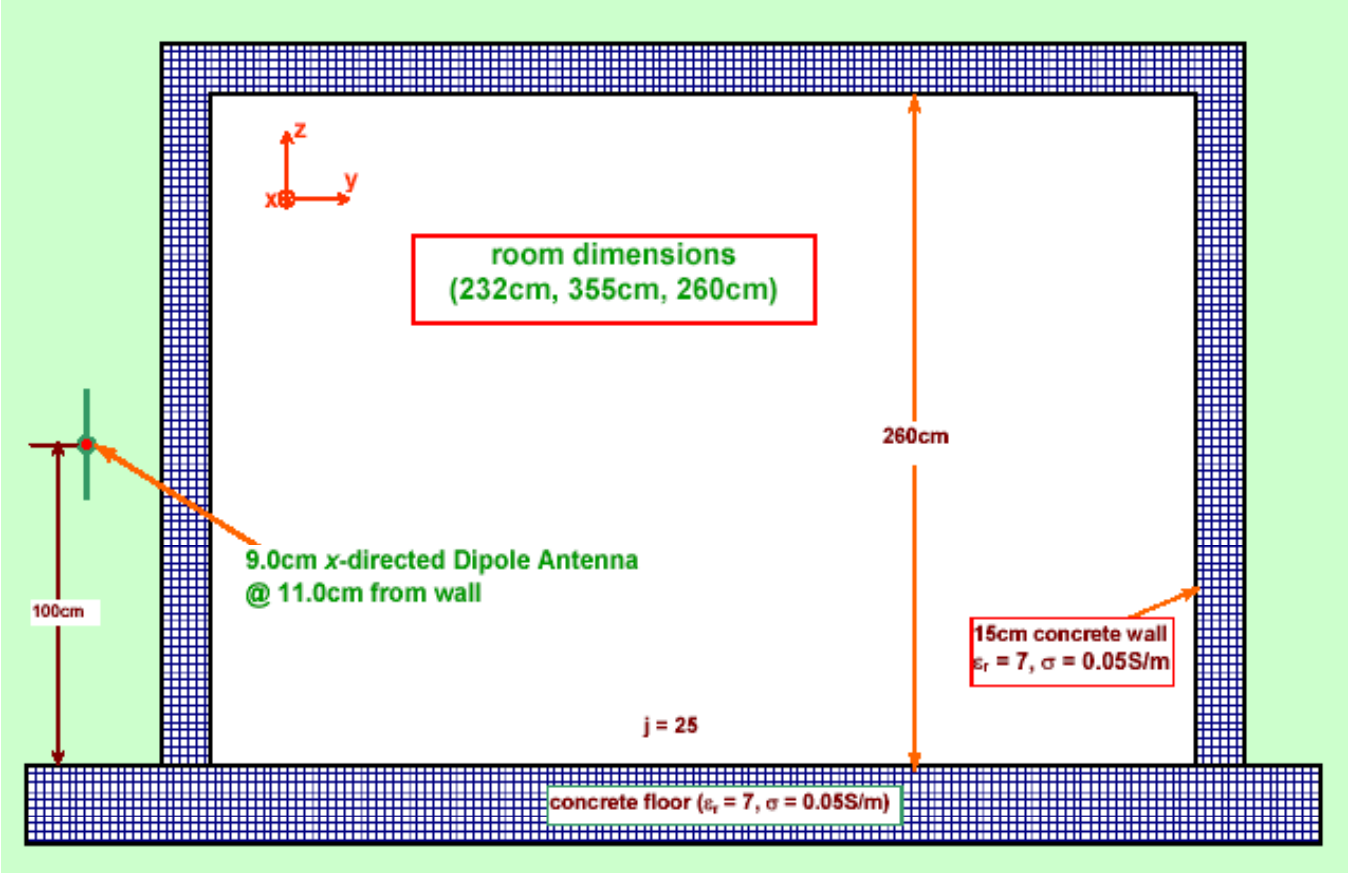

Figure 2. Side view of simulated concrete room scenario

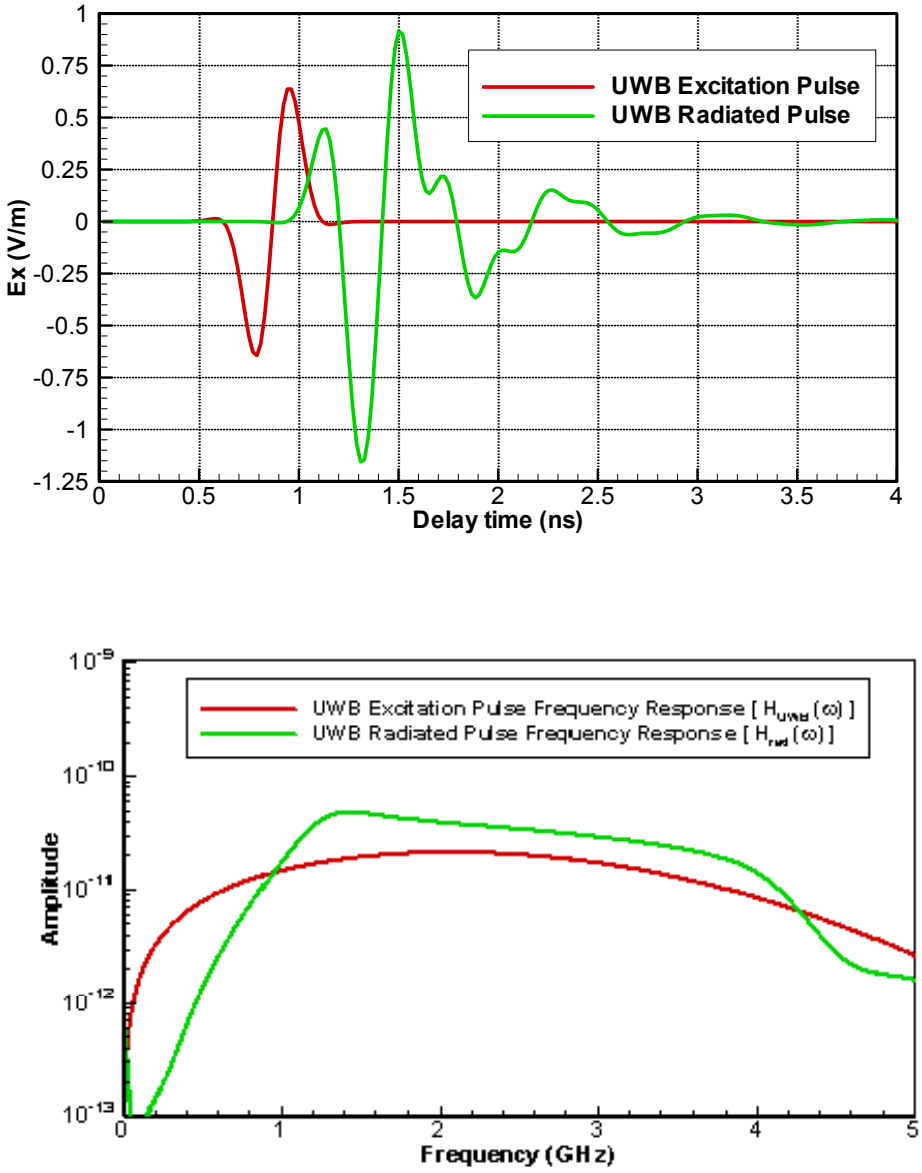

Figure 3. a) Excitation voltage pulse and UWB radiated signal; b) Frequency spectrum

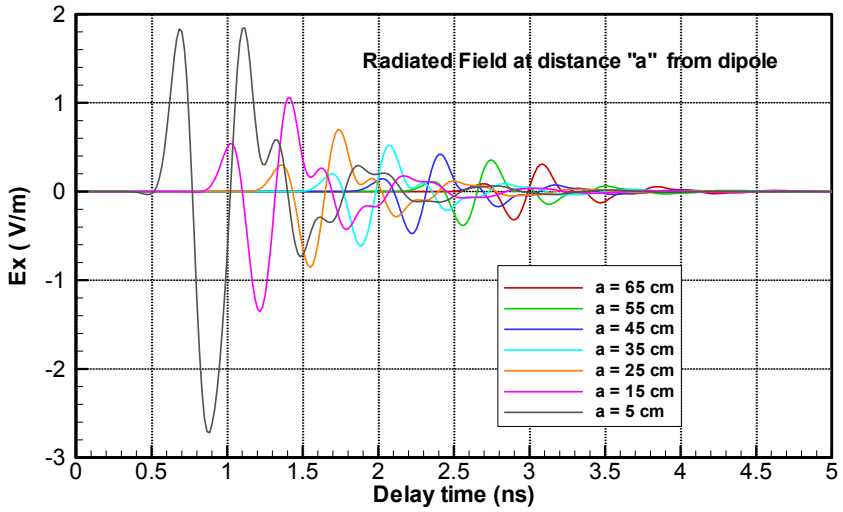

Figure 4. Radiated Field at distance 'a' from dipole

2.2 Signal propagation

UWB SP radar can provide surveillance through concrete walls only if the UWB SP signal can propagate through concrete walls. Figure 5 and 6 shows the time sequence of an UWB SP signal that is transmitted in front of a room with concrete walls. Figure 5 shows that the UWB SP signal propagates through the concrete wall to the interior of the room. Figure 6 shows part of the wave being reflected by the targets. These reflections make it possible to track the targets moving inside the concrete room. As expected, the front of the wave outside the room lags behind the one inside the room. This phenomenon will be visible on the through wall radar images especially in static mapping. Figure 7 shows that the wave front reconstructs itself after hitting the metallic cubes due to diffraction.

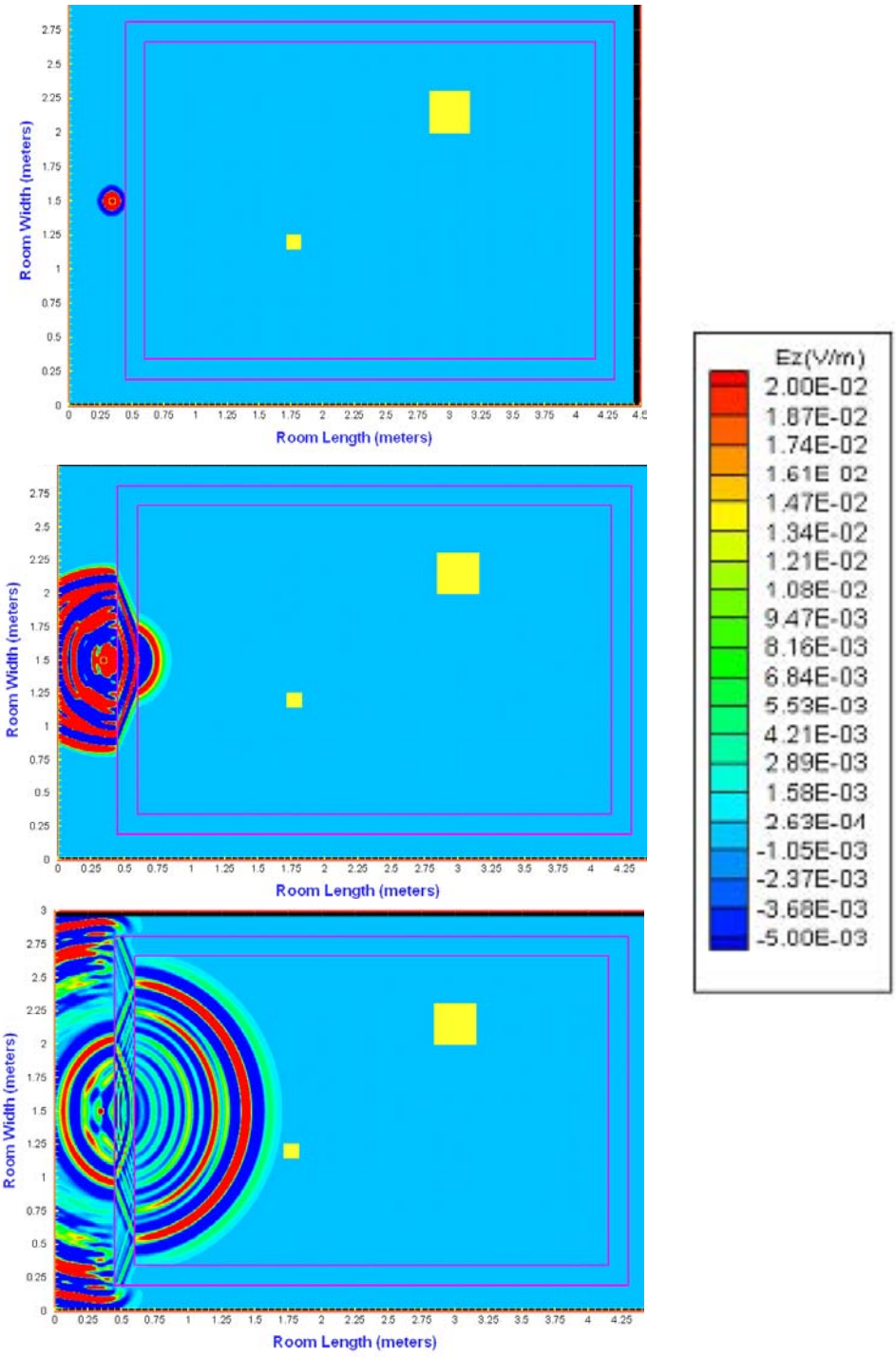

Figure 5. Time sequence of signal propagation through concrete walls

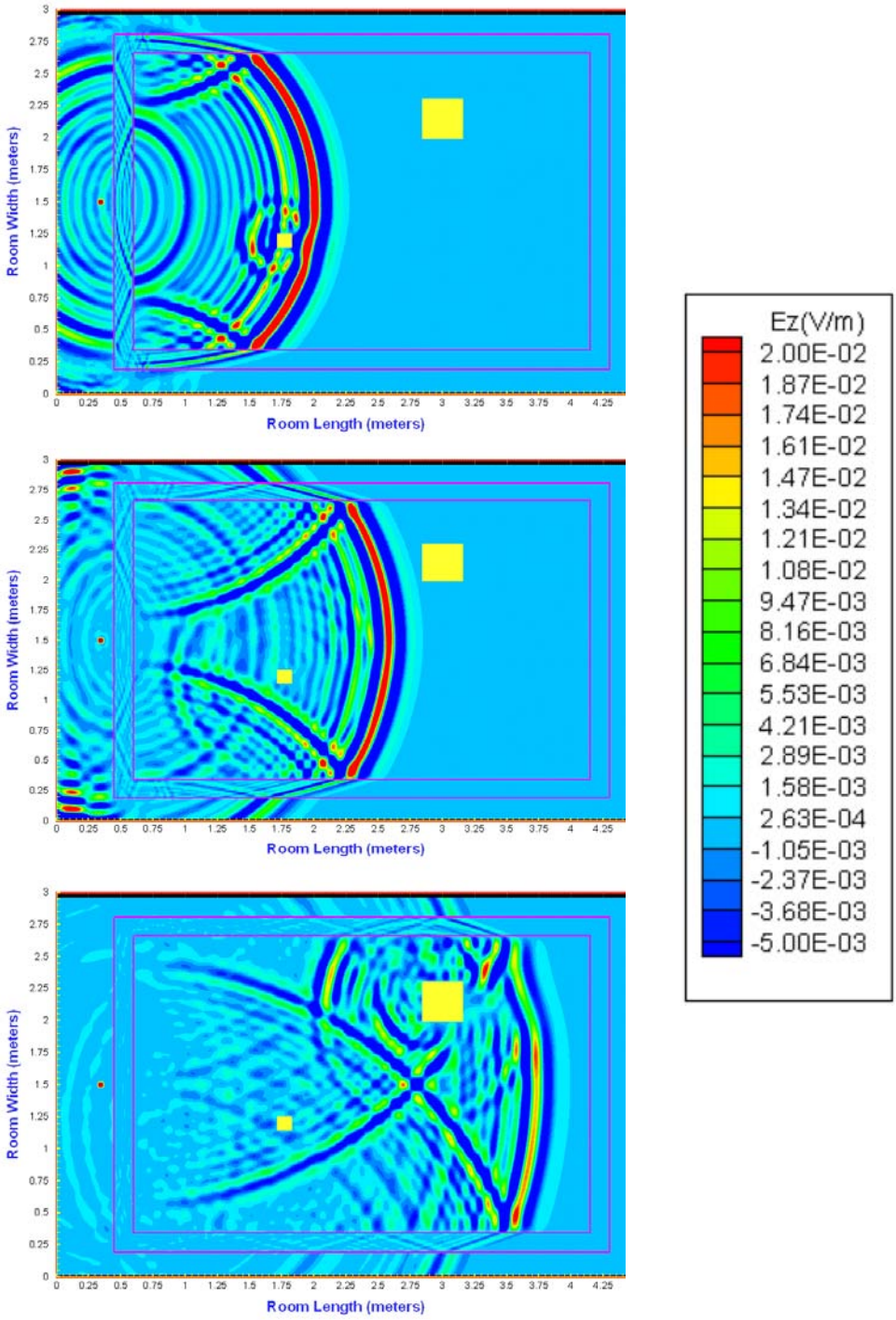

Figure 6. Signal propagation in concrete room showing backscattering of conductors

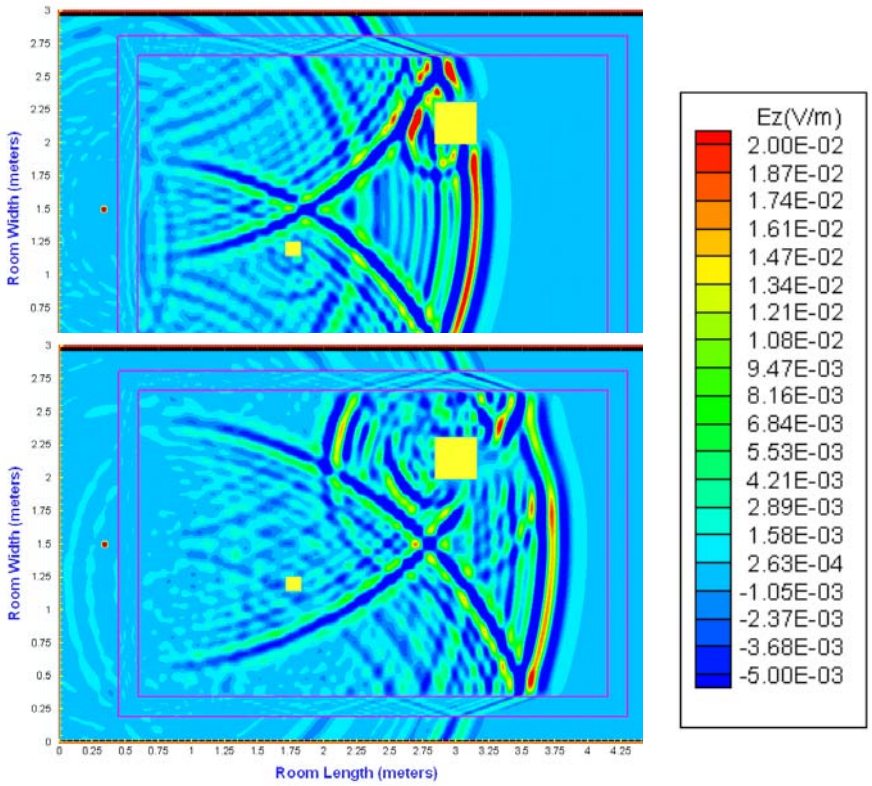

Figure 7. Signal propagation sequence showing wave front reconstruction behind target.

2.3 Received signals

Figure 8 shows examples of the signal that is received by receiver #23 on array #1 for boxes at positions 1 and 3. The displacement of the boxes cannot be determined from these two figures. In fact, the signal received directly from the transmitting antenna is much larger than any of the other echoes. This makes it difficult to see anything other than the direct signal. The direct coupling between the transmitting and receiving antennas can be removed by subtracting the return from one frame from the following one, which is a standard procedure performed in Moving Target Indicator (MTI) processing. Frame-to-frame subtraction also removes clutter coming from fixed objects since they should produce the same response from frame to frame. Figure 9 shows examples of the remaining signal after frame-to-frame subtraction when the boxes move from position 1 to 3. The two boxes are now clearly visible even though their amplitude is 100 times smaller than the fixed clutter. The displacement of the boxes from position 1 to 3 is clearly shown. The receiver time has been converted into distance traveled by determining the distance the signal travels in free space during that time. This distance represents the time taken for the signal to travel from the transmitting antenna to the target and then back to the receiver. Subtraction of the empty room response can also be used to remove most of the fixed object clutter. The fixed clutter part that is not removed is due to the clutter interaction with the targets. This residual clutter shows up as small fluctuations behind the moving targets responses [3].

Figure 10 shows the top view of the signals received at each receiver of array 1 with and without the concrete room or the targets. The receivers are distributed along the vertical axis and the horizontal axis gives the distance of the corresponding range bin. For the first frame there are no targets and no concrete room. The signal coming directly from the transmitting antennas is clearly visible in all receivers. Reflection from the ground shows up at about 2 m in all the frames of Figure 10. This distance corresponds to the distance traveled from the transmitting antenna to the ground and back to receiver element. For the second frame, the concrete room is included in the simulation. The position of the back wall is clearly visible in the reflected echoes, but the position of the front wall is not as obvious. The sidewalls do not produce back reflection since they behave like flat mirrors that reflect the wave away from the receivers of array 1. For the third frame, the two boxes at position 5 are included, but not the concrete room. The received signals are echoes coming from the two boxes at about 3.9 and 5.9m. Once again this distance corresponds to the total traveled distance from the transmitter to each box and back to the receiver. For frame 4, both the targets and the concrete walls are included. In this case, echoes from the two boxes are also visible in the received signals but are little farther away than expected. This is due to the delay of the EM signal inside the concrete walls. The presence of concrete walls reduces the amplitudes of the echoes returning from the boxes. Figure 11 shows the top view of the moving target signals obtained by subtracting all received signals with boxes at one position and then at another position. The boxes have different positions from frame-to-frame to simulate motion. The frame-to-frame subtraction removes clutter from fixed objects as well as direct coupling from the transmitting antenna. Hence only the responses from the moving targets are visible in the figure. The above results show that the received signal can provide information about the illuminated scene without any special processing. The transformation of the received signals into radar images is the subject of the next section on image generation algorithms.

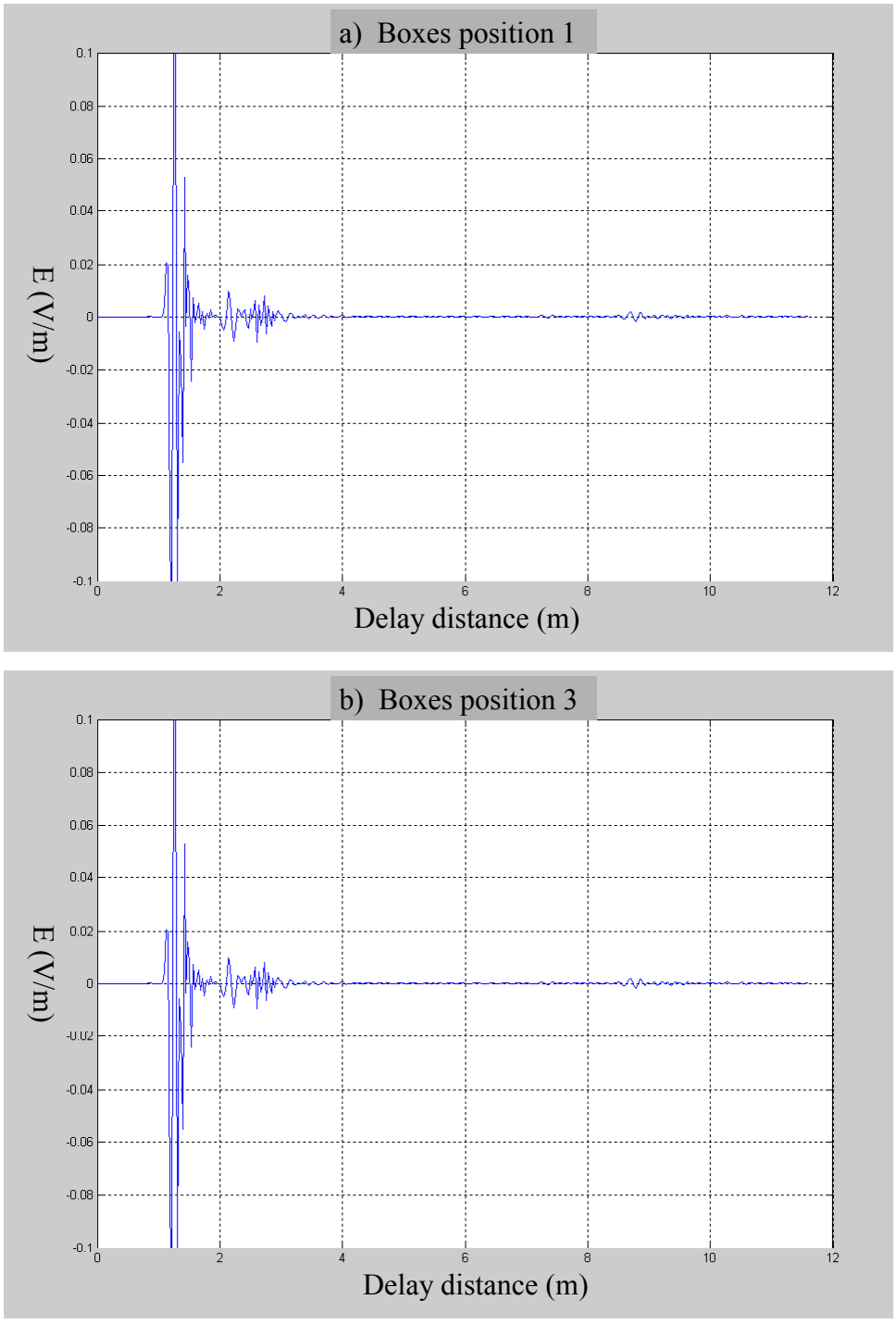

Figure 8. Received signal at receiver 23 for boxes position 1 and 3

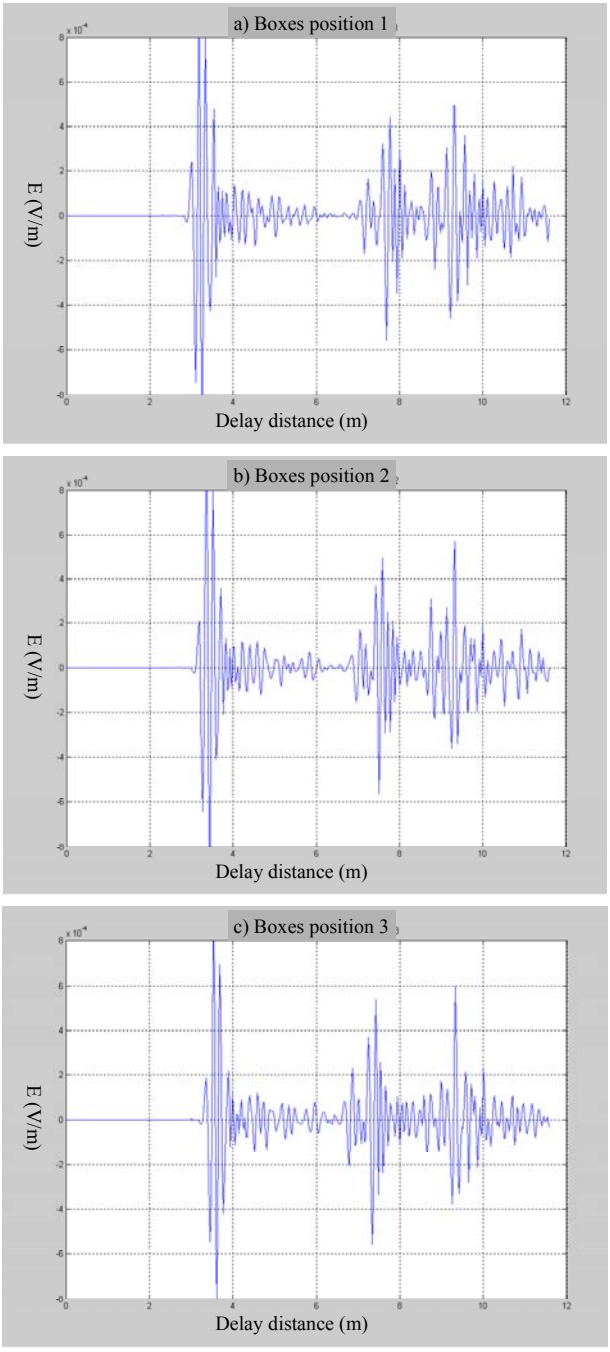

Figure 9. Pulse to pulse subtraction of received signal at receiver 23 for boxes position 1, 2 and 3

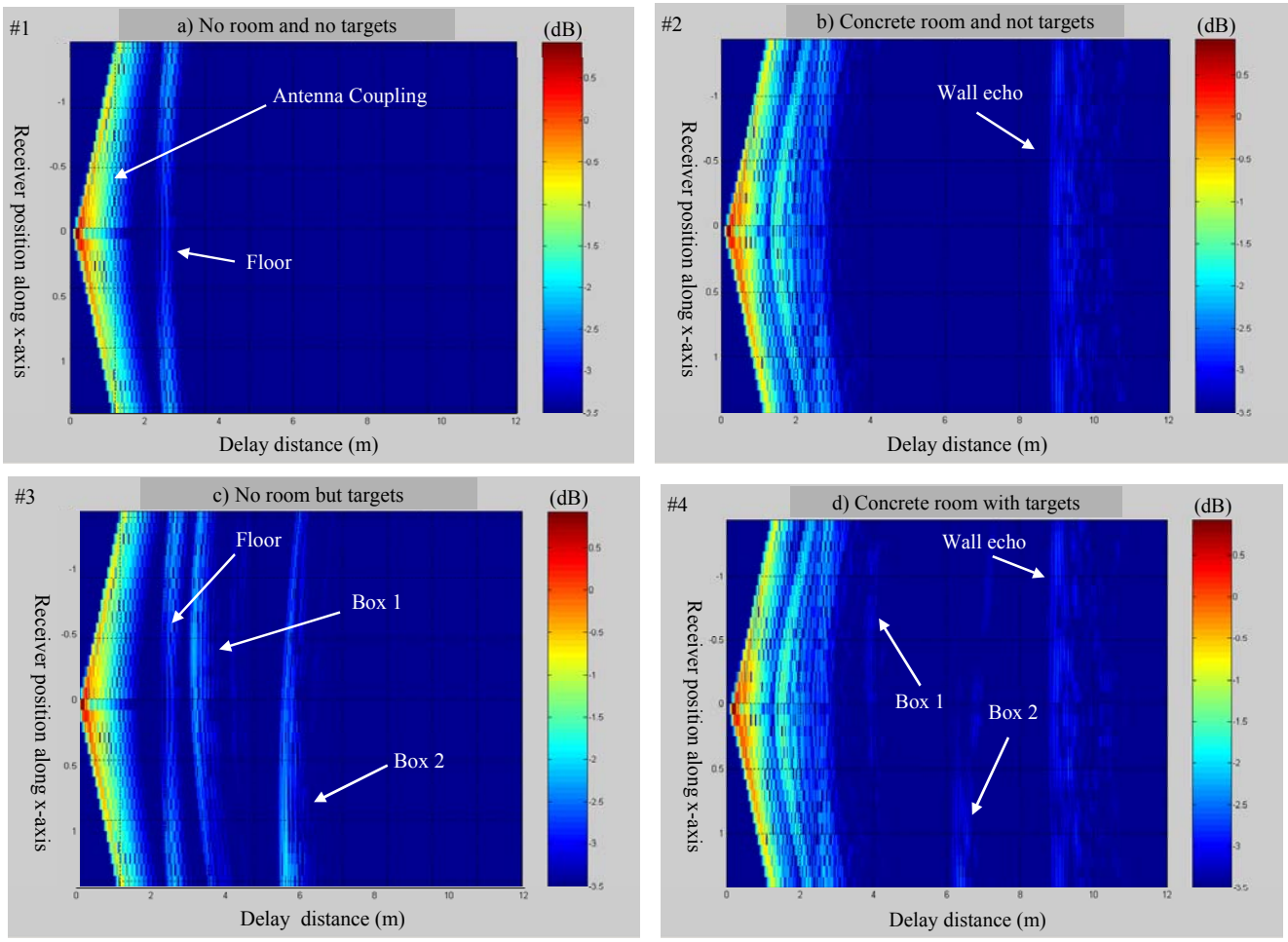

Figure 10. Top view of signal received at each receiver

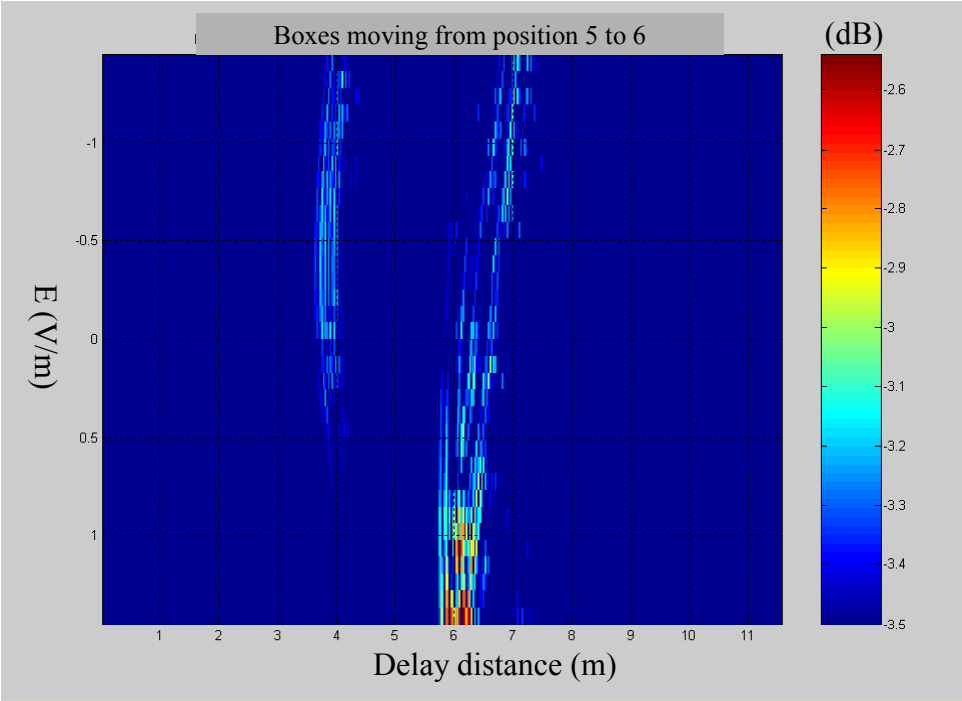

Figure 11. Signal differences from subsequent frames showing the echoes of the two moving boxes

3. Radar imaging algorithms

The image generation algorithm used in this report is based on the back projection technique [3]. The same algorithm is used to produce radar images of static objects as well as moving targets. For the moving targets, however, clutter from fixed objects is first removed from the received signals. This is done by subtracting the received signals from subsequent frames or from the received responses of an empty room.

3.1 Back projection algorithm

The data from each received signal consists of a set of electric field values as a function of the time traveled by the radar signals. The signal received at a given time can be from all pixel locations where the total flight time is equal to this specific time bin. The total flight time is the time to travel from the transmitting antenna to the pixel and then back to a receiver. Figure 12 shows examples of pixel location where the reflected signal can come from for a set of collocated transmitting and receiving antenna elements. The back projection technique consists of recording the amplitude of each time bin on a spatial grid based on the total flight time. After that, all the recorded amplitudes from each channel are added together on the spatial grid. At the target locations the signal amplitudes will add up coherently and should build up quickly. The back projection algorithm has been implemented as follows:

1) Divide the whole region to be divided into small surface areas or pixels;
2) For each pixel, calculate the total flight time from transmitter to pixel and pixel to a receiver;
3) Record the corresponding received time bin amplitude for each pixel.
4) Repeat step 2 and 3 for all receivers;
5) Sum the recorded amplitudes on the spatial grid.

Mathematically, in free space, the back projected signal at pixel (x_i, y_i) in the room image plane is given by:

$$I(x_i, y_i) = \sum_n E[t_i(n), n] \tag{1}$$

where,

$$t_i = (T_i + R_i(n))/c \tag{2}$$

$$T_i = \sqrt{(x_i - x_T)^2 + (y_i - y_T)^2} \tag{3}$$

$$R_i(n) = \sqrt{(x_i - x_R(n))^2 + (y_i - y_R(n))^2} \tag{4}$$

where:
c is the speed of light in free space (m/s); I is in V/m; t in second; x, y, T and R in meter.

$t_i(n)$ is the total time for the transmitted signal to travel to pixel (x_i, y_i), which is T_i, and then travel back to receiver n, which is $R_i(n)$.

The set $\{x_T, y_T\}$ are the coordinates of the transmitter and the set $\{x_R(n), y_R(n)\}$ are the coordinates of the nth receiver. The result of this procedure is a 2D radar image, which provides both range and direction of the potential targets moving behind the walls.

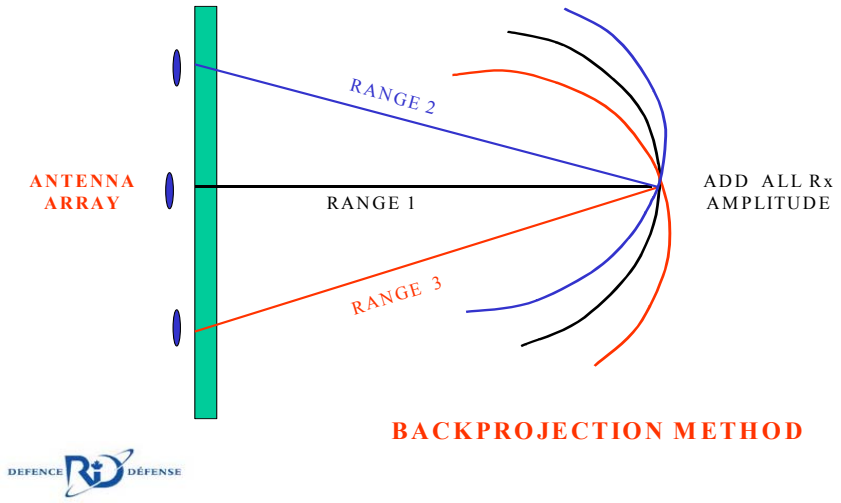

Figure 12. Antenna array and back projection technique

3.2 Correction for signal velocity inside walls

The accurate calculation of the total flight time is a critical step in the back projection algorithm. The velocity of the signal inside concrete walls is slower than in free space. This will result in longer flight time for a given set of transmitter, pixel and receiver locations. In this report, the effects of refraction are ignored. Radar images obtained using only velocity correction show that refraction has little impact.

The time for a radar signal to travel a given distance d_{inwall} inside a wall is given by:

$$t_{inwall} = \frac{d_{inwalll}}{v_{wall}} \tag{5}$$

where v_{wall} is the velocity of the signal inside the wall. The velocity of the electromagnetic signal is related to the wall permittivity and permeability as follows [15]:

$$
\begin{aligned}
v_{wall} &= \frac{1}{\sqrt{\mu_{wall}\ \varepsilon_{wall}}} \\
&= \frac{1}{\sqrt{\mu_0 \varepsilon_0\ \mu_{r\_wall}\ \varepsilon_{r\_wall}}} \\
&= \frac{c}{\sqrt{\mu_{r\_wall}\ \varepsilon_{r\_wall}}}
\end{aligned}
\tag{6}
$$

where:

c is the speed of light in free space,
μ_{wall} and ε_{wall} are the permeability and permittivity of the wall,
μ_0 and ε_0 are the permeability and permittivity of free space,
μ_{r_wall} and ε_{r_wall} are the relative permeability and permittivity of the wall.

For non-magnetic materials such as concrete, the relative permeability is equal to one. Hence for concrete walls,

$$
v_{wall} = \frac{c}{\sqrt{\varepsilon_{r\_wall}}} \tag{7}
$$

By substitution,

$$
t_{inwall} = \frac{\sqrt{\varepsilon_r}\ d_{inwall}}{c} \tag{8}
$$

The delay time through concrete walls compared to free space propagation is determined by

$$
\begin{aligned}
t_{delay} &= \frac{d_{inwall}}{v_{wall}} - \frac{d_{inwall}}{c} \\
&= \frac{d_{inwall}}{c} (\sqrt{\varepsilon_{wall}} - 1)
\end{aligned}
\tag{9}
$$

The permittivity of concrete is set to the standard level of seven to generate the simulated data. The distance traveled inside the concrete walls is required to determine the difference in travel time with respect to free space due to the walls. This calculation of the distance traveled inside concrete wall is implemented as follows:

1) Connect a line between the position of the transmitter (or receiver) and the pixel (x, y). See Figure 13.
2) Find the intersection points with the external walls of the room using slope of this line
3) Calculate the distance traveled inside that box using intersection points
4) Find intersection points with the internal walls of the room using slope of the line going from the pixel to the receiver
5) Calculate the distance traveled inside that box using intersection points
6) The differences between the distances traveled in the large and small box (the external and internal walls lines respectively) give the total distance traveled inside the concrete wall.

This technique makes it possible to correct for the signal velocity through all of the walls. The wall coordinates are shown in Figure 1. Hence, the travel time difference due to concrete walls can be calculated and included into the back projection algorithm.

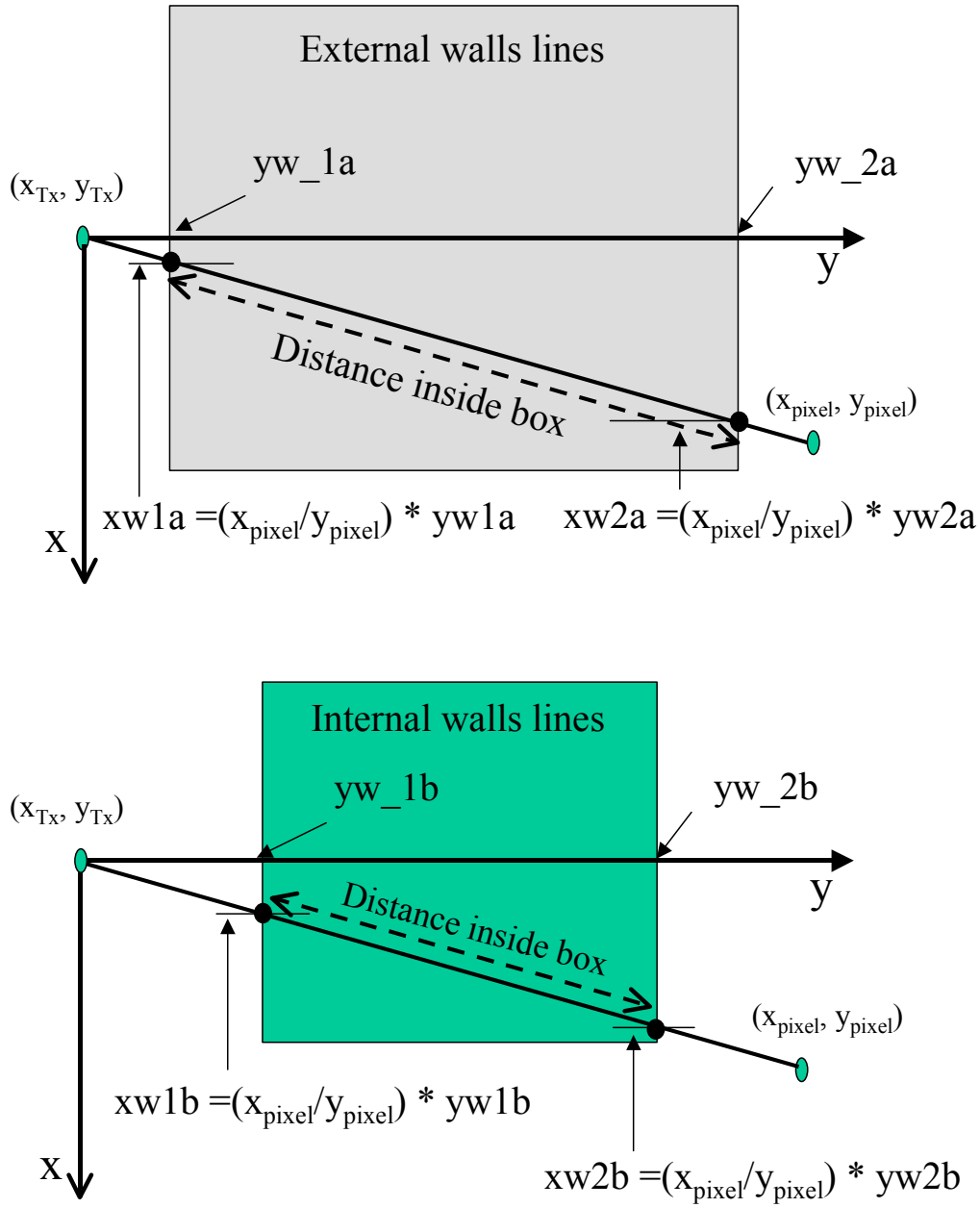

Figure 13. Calculation of the distance traveled through walls

4. Moving targets

This section examines the capability of UWB SP radar for providing through concrete wall imaging of moving targets. Unless otherwise specified, the stationary clutter has been removed by subtraction using the empty room response. MTI-like radar processing is more realistic of real field operation. However, in the simulated data, most of the targets displaced are by 10 cm steps, which does not produce good radar images using MTI techniques. Subtraction with the empty room is representative of the best radar images that can be obtained using MTI-like radar techniques, i.e., if target displacement between frames is small enough.

4.1 Moving targets imaging

This sub-section produces radar images of the moving targets without correcting for the propagation phenomenon due to the concrete walls. In other words, all of the received signals are processed assuming free space characteristics.

Figure 14 shows radar images of the boxes at positions 1 and 5 respectively, with and without concrete walls. The radar blobs represent the radar images of the moving targets. The initial position of the boxes, antenna elements and concrete walls has been superimposed on these figures to emphasize the impact of concrete walls on the radar images. The first two frames clearly show that UWB SP radar is capable of tracking moving targets behind a concrete wall.

Concrete walls have three distinct impacts on the radar images: Firstly, the radar targets are displaced away from their true positions. This is due to the signal velocity decrease due to the concrete wall. Secondly, the target images are significantly defocused as compared to the "no walls" case. Thirdly, the radar images created with concrete walls produce false targets outside of the room. The false target behind the back wall is due to shadowing of the target on that wall. The other false target was originally thought to be caused by a reflection on the concrete wall. However, this was not the case as will be shown in the next sub-section. A close look at the "no walls" figures show that even without walls the radar targets are slightly lagging their true position (≈10cm). This is due to the limited bandwidth of the transmitting dipole antenna, which limits the antenna response time. If a de-convolution is first performed on the received signals and the antenna response then the positions of the radar targets will coincide with their true position [4].

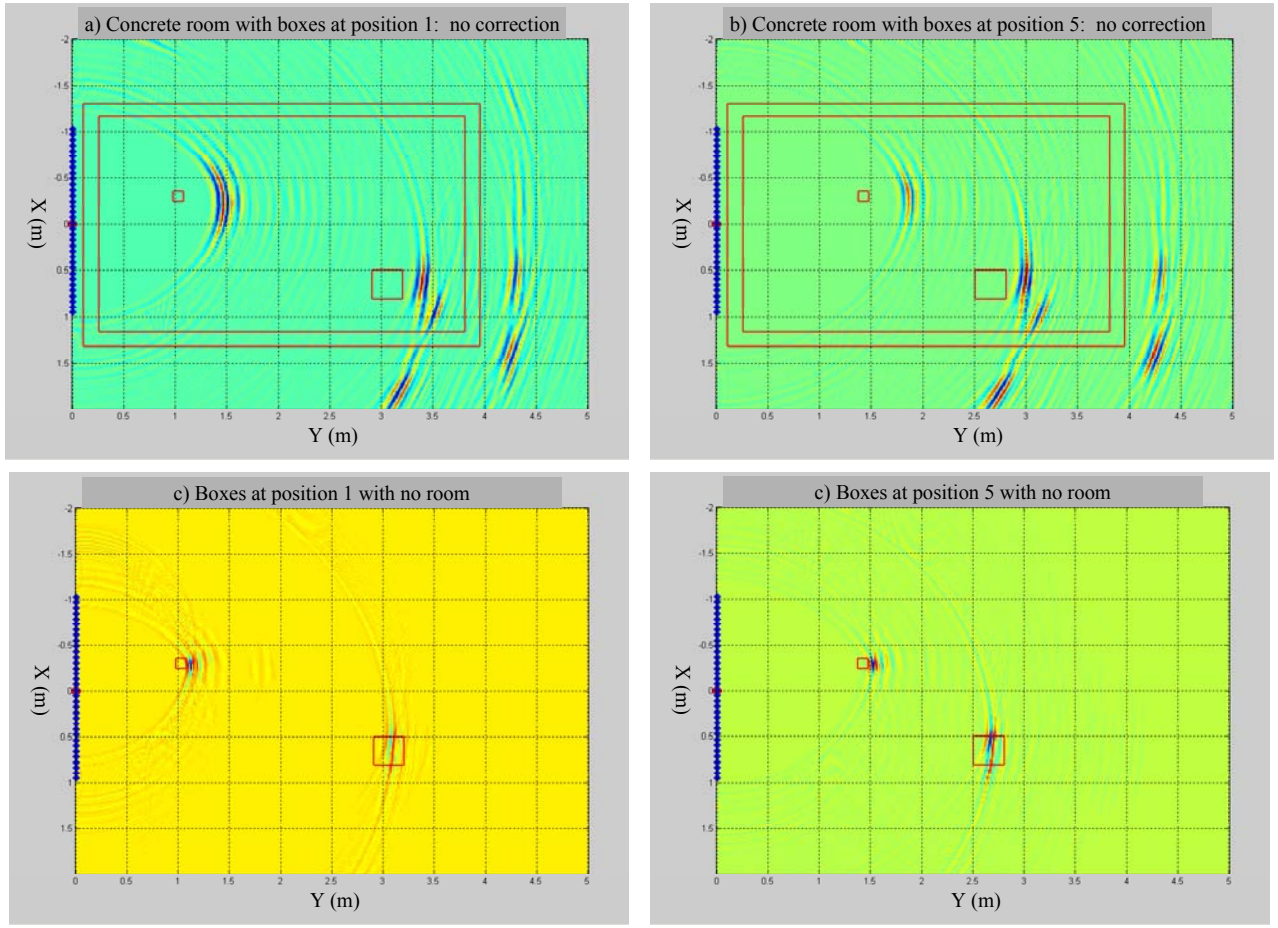

Figure 14. Radar Images of the moving boxes with and without the concrete room

4.2 Refocus radar images

This sub-section examines the benefit of considering the travel time differences due to propagation through concrete walls into the image generation algorithm.

Figure 15 shows the radar images of moving boxes obtained without velocity correction, with correction for the front wall, with correction for all walls and finally without a concrete room. Correcting for signal velocity for only the front wall will only refocus the images of the targets inside the room and should bring them closer to their true position. Correcting for velocity through all the walls should reduce the shadow on the back wall. This will also transform the false target outside the room into the box image's side-lobe. Figure 16 shows an example of the target side-lobe existing outside the room. This was obtained using a smaller antenna aperture size. The target side-lobes are not circular as in free space. In fact, the electromagnetic wave front propagating outside the room lags behind the wave inside the room (Figure 17). This is due to the slower signal velocity inside the concrete walls. The region corresponding to a given flight time is not circular anymore, as is the case in free space. In Figure 15 the radar images obtained using velocity correction are comparable in quality to the no walls case. Hence there is no real need to correct for the refractive effects as is done in references [10 and 13]. This is interesting since correcting refractive effects require much more processing time. In summary, velocity correction considerably improves the quality of the radar images.

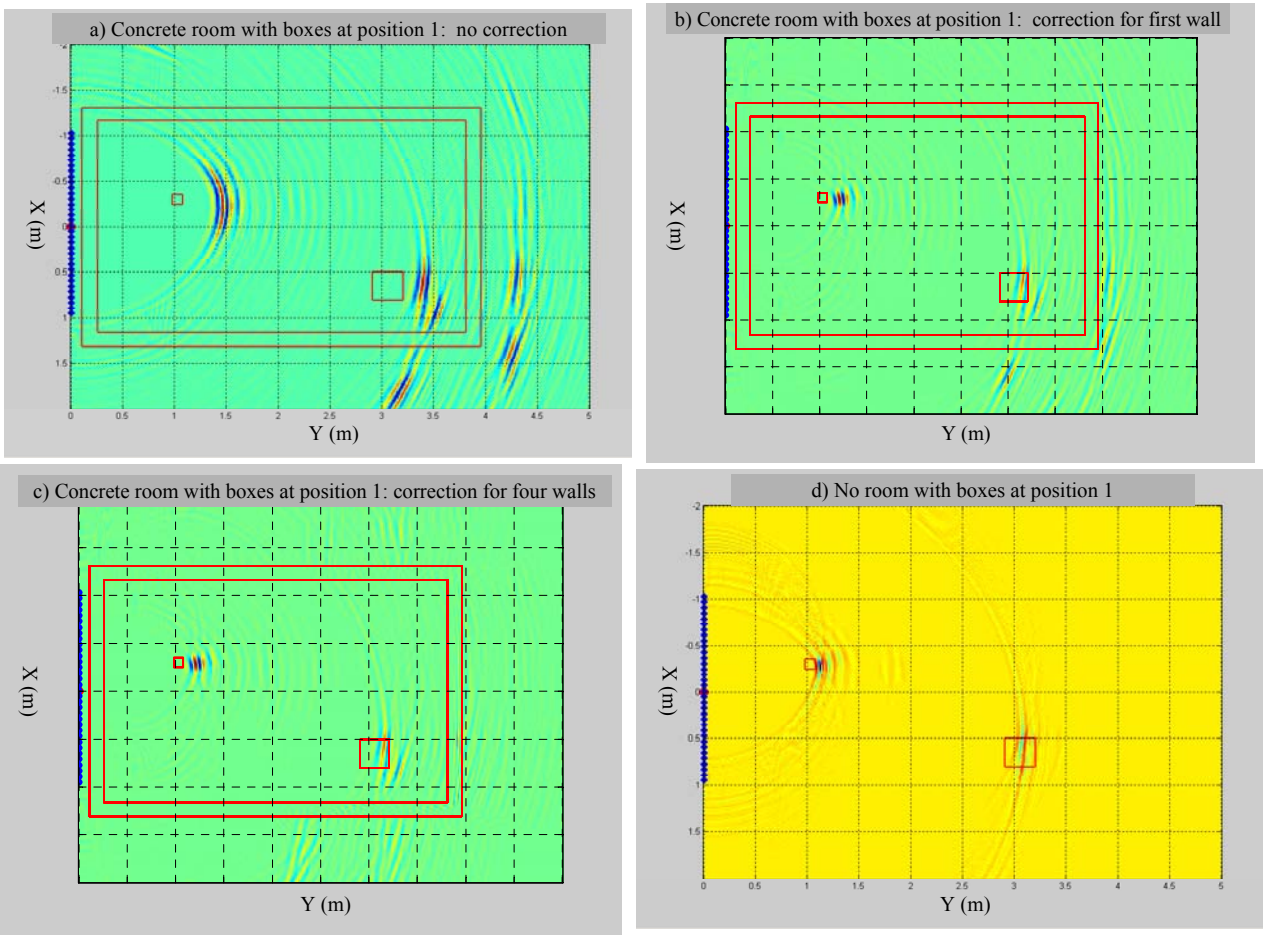

Figure 15. Receiver array size of 2m: a) no correction; b) correction for first wall; c) correction for all walls; d) no walls case

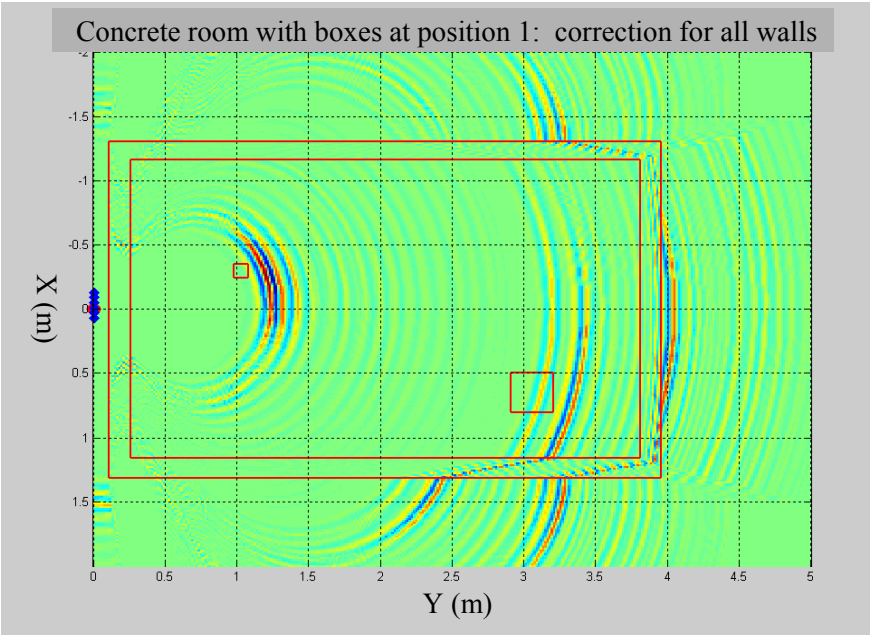

Figure 16. Example of target image side lobes going outside the room (Antenna array size 20cm)

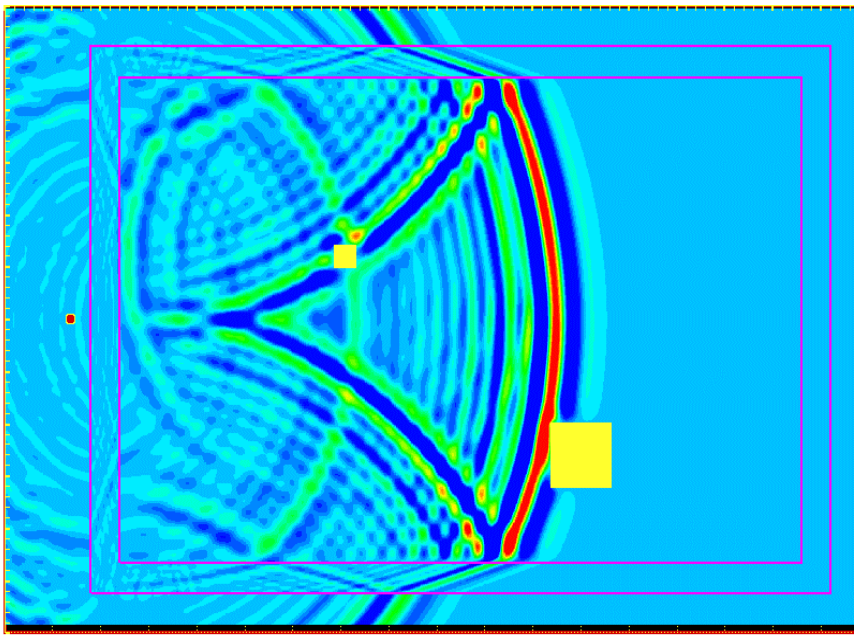

Figure 17. Electromagnetic wave propagation into concrete room

4.3 Clutter suppression techniques

This sub-section compares the radar images of moving targets obtained using subtraction of the empty room response with those obtained using frame-to-frame subtraction.

This sub-section first looks at the difference between the two-clutter suppression techniques by having only a small target displacement for the frame-to-frame, or subsequent frame, subtraction. This should produce a better comparison between both techniques.

Figure 18 (a) shows the radar images obtained by subtracting the received signals with the empty room response. Figure 18 (b) shows the radar images obtained by subtracting the received signals with the subsequent frame. The target displacement between two adjacent frames is 1 cm. The location of the boxes at the first position is indicated on the figure as well as the direction of motion. The main difference between the two images is that the image obtained using the subtraction with subsequent frames does not have a shadow on the back wall.

Intuitively, one would think that a target displacement must be larger than the radar range resolution to be detectable as a moving target. Radar range resolution is given by:

$$\Delta R = \frac{c\,\tau}{2} \tag{10}$$

where c is the speed of light and τ the pulse duration time [16]. For the simulated radar, the pulse duration is 0.5 ns, which means a range resolution of 7.5 cm. The 1 cm displacements of the targets are clearly visible on the radar images of Figure 18 b.

Figure 19 shows radar images obtained using velocity correction with the two clutter suppression techniques. It also shows the radar image for the no walls case for comparison. The radar images of the targets images are comparable in quality to the no walls clutter suppression technique.

Figure 20 shows the radar images obtained using subtraction with subsequent frames, but for target displacements of 1, 10 and 50 cm respectively. For a 10 cm target displacement, the target image seems to be longer in range. In fact, subtraction with subsequent frames shows the superposition of target response of both positions, which is separated here by 10 cm. This is obvious with the 50 cm target displacement. In this case, the targets response at each position are well separated and do not overlap.

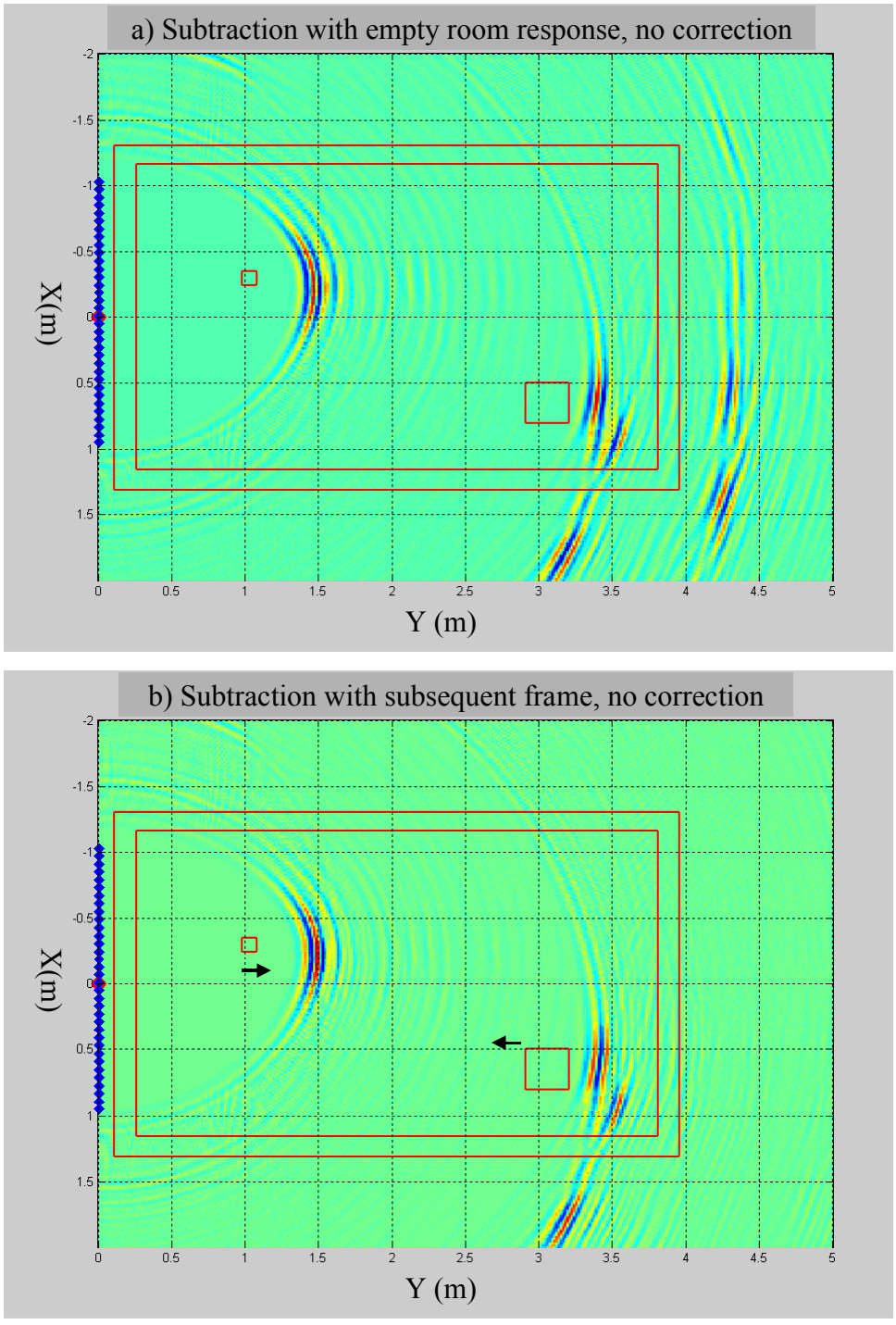

Figure 18. Subtraction with a) empty room response; b) subsequent frame (1cm target displacement).

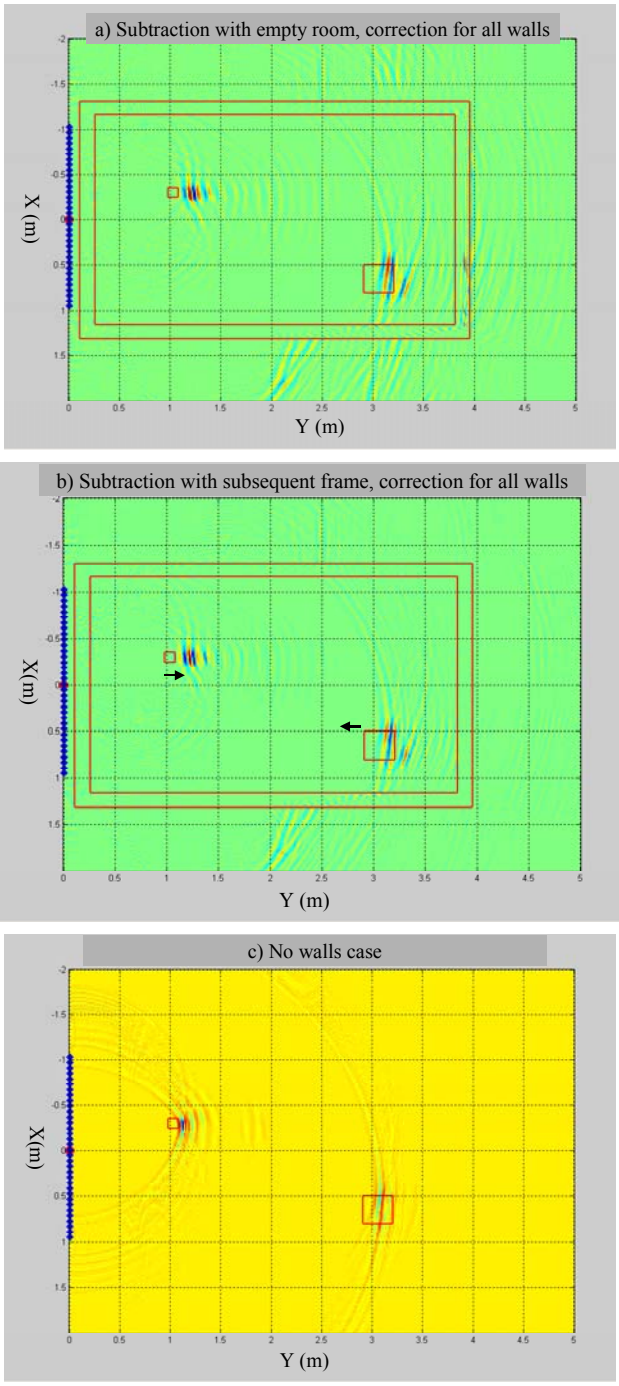

Figure 19. Subtraction with a) empty room response, b) subsequent frame and c) no walls case

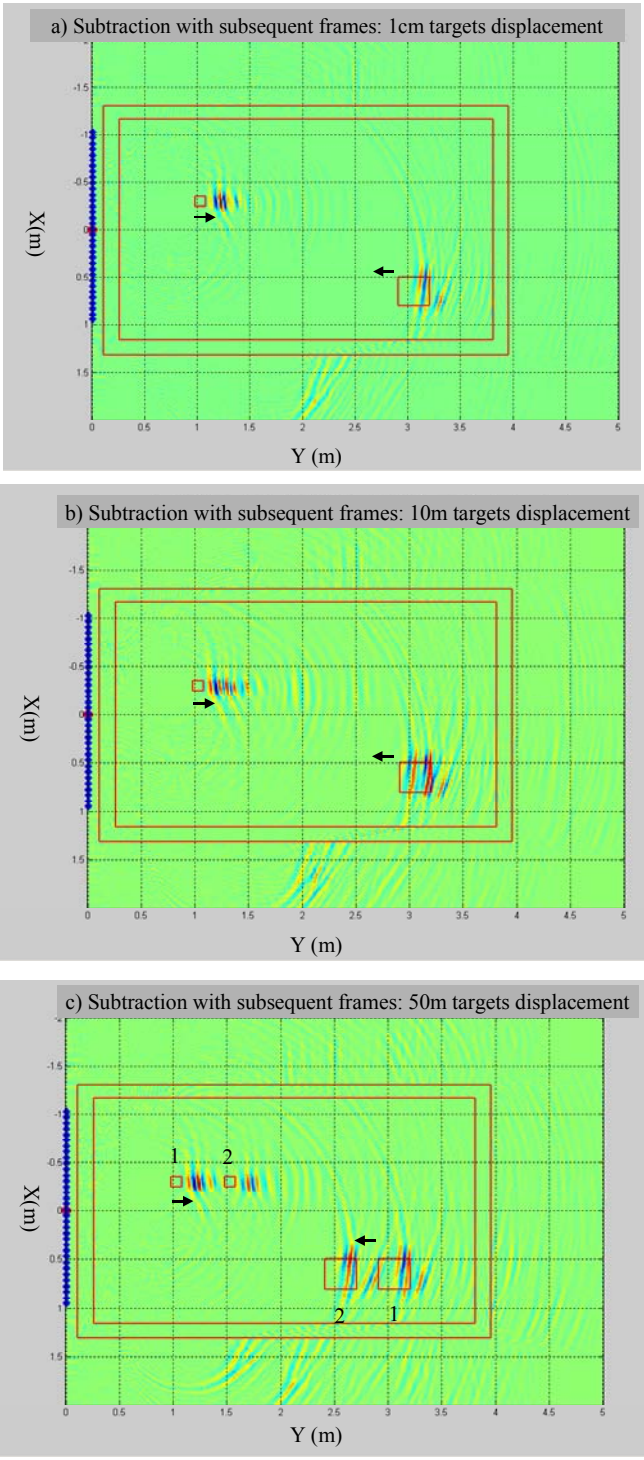

Figure 20. Radar images of moving targets with displacement of: a) 1cm; b) 10cm; c) 50cm

5. Static mapping

The radar images in this section have been obtained by applying the back projection algorithm directly on the received radar data without any pre-processing. These raw received signals include both echoes from the fixed objects and from the moving targets.

5.1 No correction

Figure 21 shows radar images obtained by using the back projection algorithm directly on the raw radar data with and without the concrete room. The first radar image does not provide any indication of the presence of the concrete walls. In fact, the radar images look the same with or without the concrete room. There are no indications of reflection from ground or walls. In fact, the signal coming directly from the transmit antenna is much stronger than any other echoes, which makes it difficult to see the smaller echoes. For example, Figure 22 shows the same picture with three different colour scales. In the first frame, the colour scale is still linear but is clipped. As a result, the reflection on the ground around 1 m and the back wall are visible as well as the coupling between the antennas. The side walls are not visible since incident signals are only reflected forward and cannot be seen with the back receiver. The second frame uses a logarithmic colour scale that produces the same effects but with better imaging quality. The third frame also uses a logarithmic scale but only shows the amplitude values above a threshold of –2.5 dB. This produces cleaner radar images and keeps only the most relevant information, such as the wall position. Another technique to improve the visibility of small targets is by correcting for the spherical spreading. This is done by multiplying the signal amplitude with the corresponding distance, compensating for the signal energy decay as the square of the distance. This technique was used in references [10, 13] but not in this report.

Figure 23 shows the radar display for static mapping of three cases: no walls, concrete room and concrete room where direct coupling has been subtracted. In the first frame, the direct signal coupling from the transmit antenna into the receiving antenna is very strong. The reflection from the ground at about 1 m is also visible. In the second frame, for the concrete room, the direct coupling and ground reflection are still visible. However, the direct coupling pattern has changed due to the front wall that produces reflection overlapping with the direct signal. The back wall is clearly visible but the front wall is not clearly visible due to being in the direct coupling region. In the third frame, the received signals have been subtracted from the no-wall case to remove the direct coupling from the transmitting antenna. This had no obvious effect. Figure 24 uses a smaller value of pixel amplitude with and without direct coupling and there is still no obvious difference in the displayed images. The direct coupling has only been reduced in the region very close to the transmitting antenna. Since the direct coupling is not the same with and without the walls, it cannot be subtracted efficiently.

Figure 25 shows the time sequence of the moving boxes using static mapping. In these cases the targets are clearly visible as well as their displacement from frame-to-frame. Hence, UWB SP radar as defined can be used to provide static mapping of the room layout including the targets.

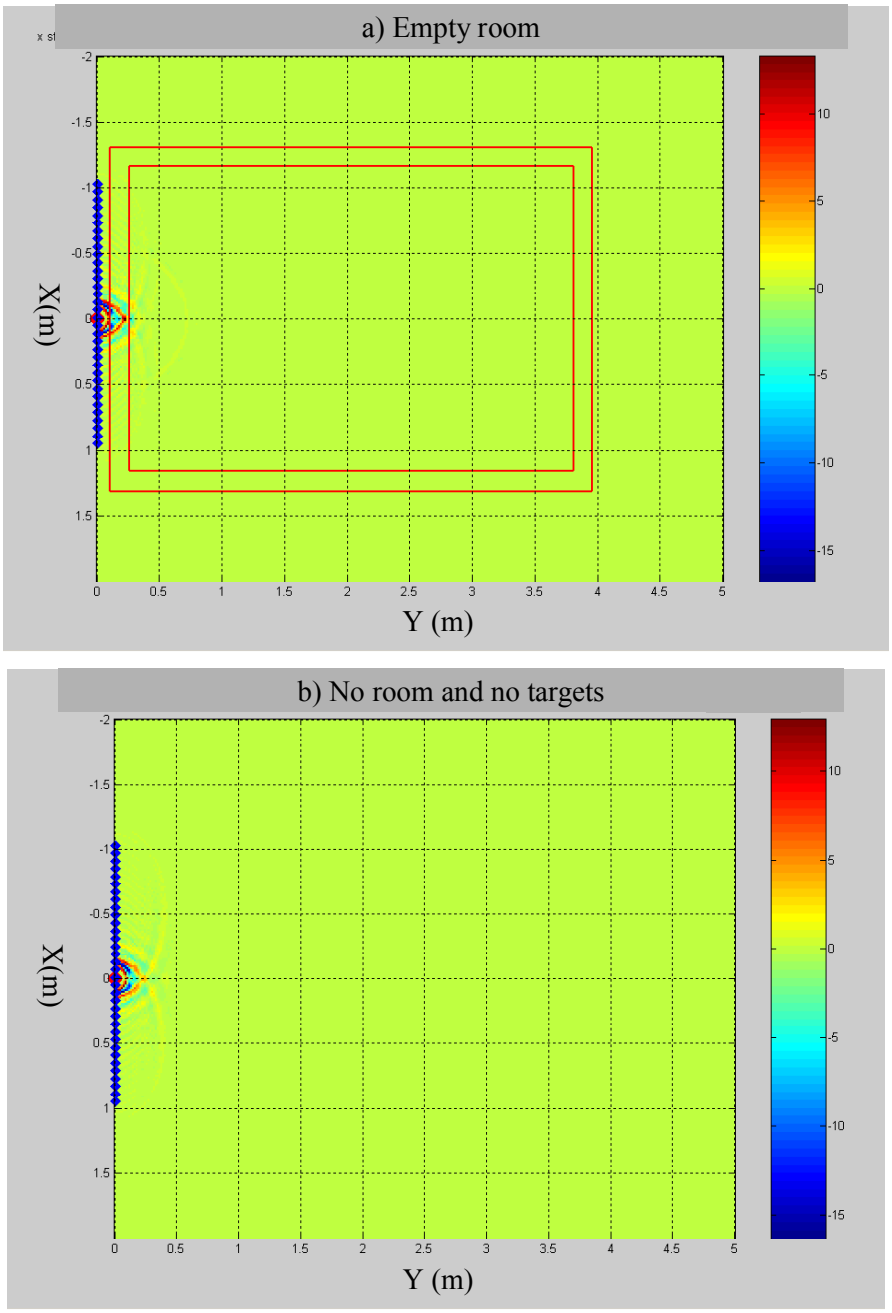

Figure 21. Static mapping with and without concrete room.

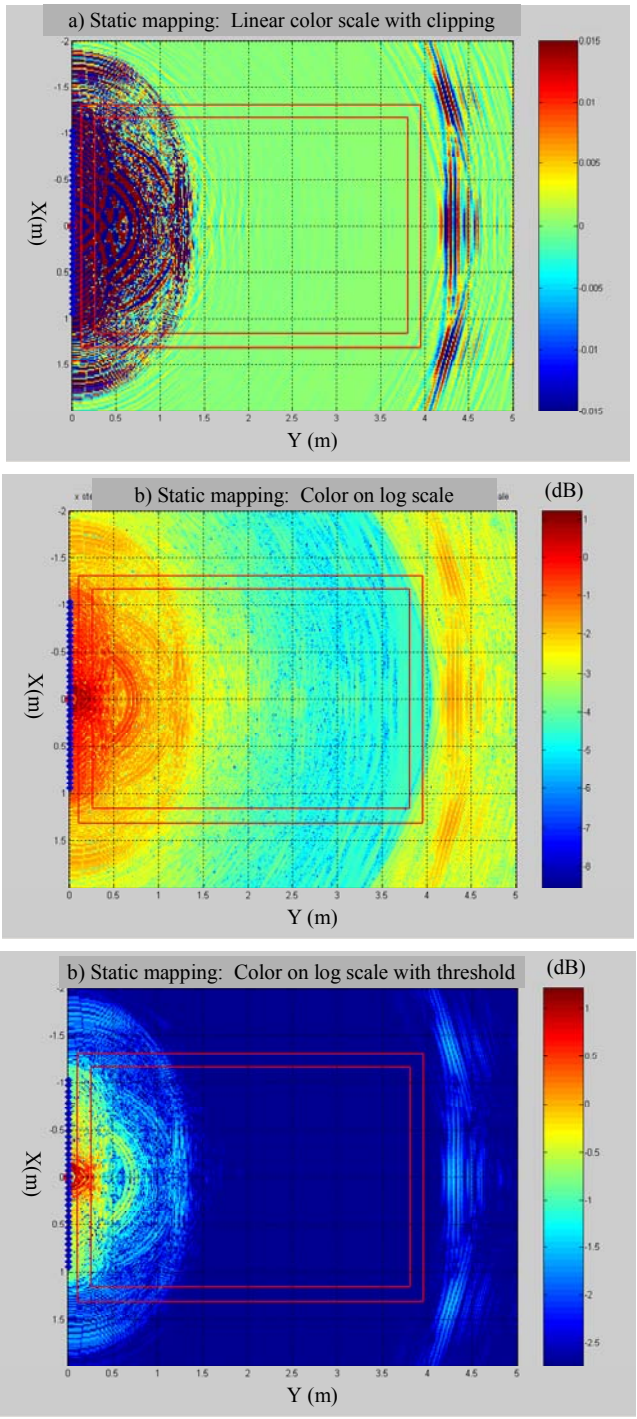

Figure 22. a) Linear colour scale with clipping; b) Colour on log scale and c) same with threshold

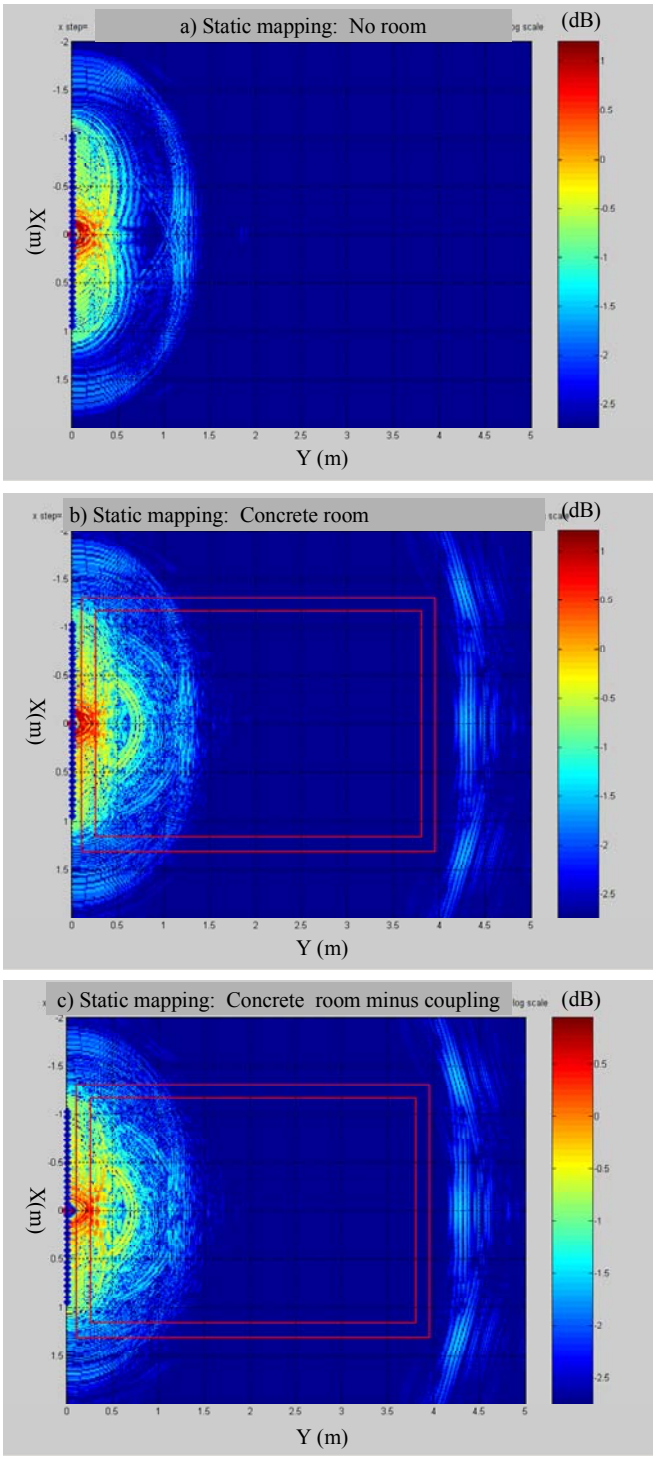

Figure 23. Static mapping: a) no room, b) concrete room and c) concrete room minus coupling

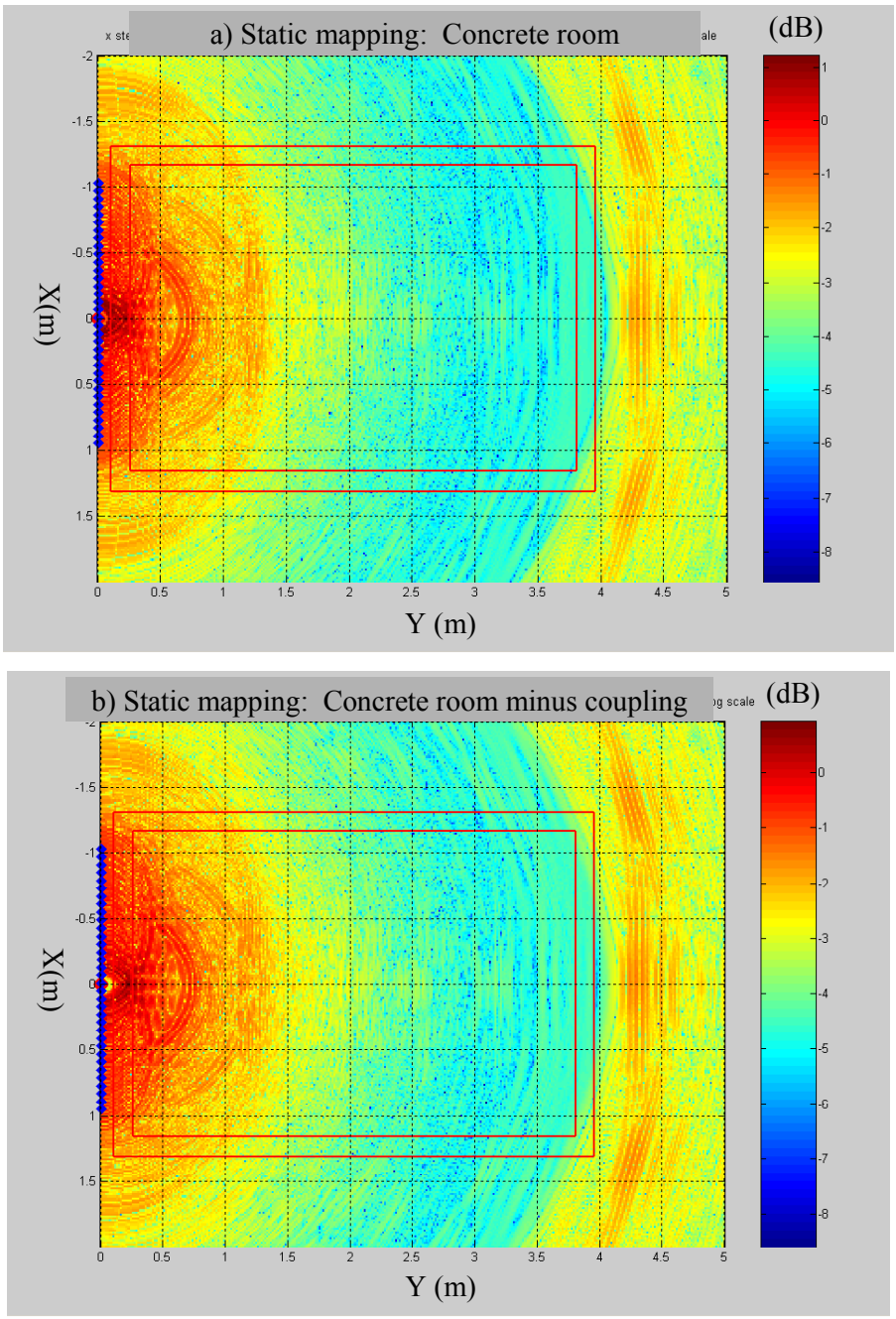

Figure 24. Static mapping of concrete room with and without direct coupling.

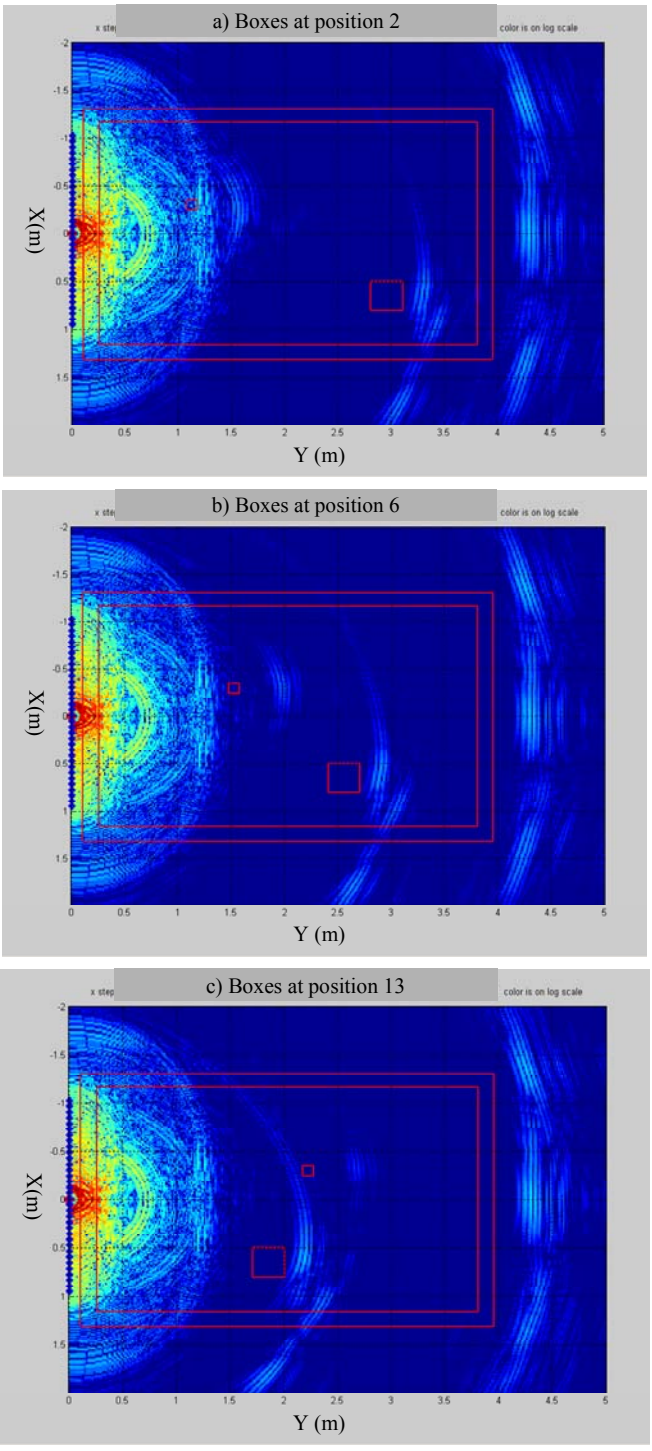

Figure 25. Static mapping of concrete room with boxes at different positions: No correction

5.2 Static mapping obtained with signal velocity correction

Figure 26 shows a radar display of static mapping without velocity correction, with correction for the front wall and with correction for all the walls, respectively. Results are similar to the moving targets cases. Without velocity corrections, the back wall and targets are displaced from their true positions. When correcting velocity for the front wall, the radar images of the targets and back wall are closer to their true positions and the target images are also much more focused. The direct coupling region also changed significantly with velocity correction. When velocity is corrected for all walls, the back wall and targets images are even closer to their true positions. The side lobes of the back wall and the large box images extend outside the room behind the target images. These side lobes are no longer parabolic as in free space. This is due to the way the wave propagates inside and outside the room as shown in Figure 17.

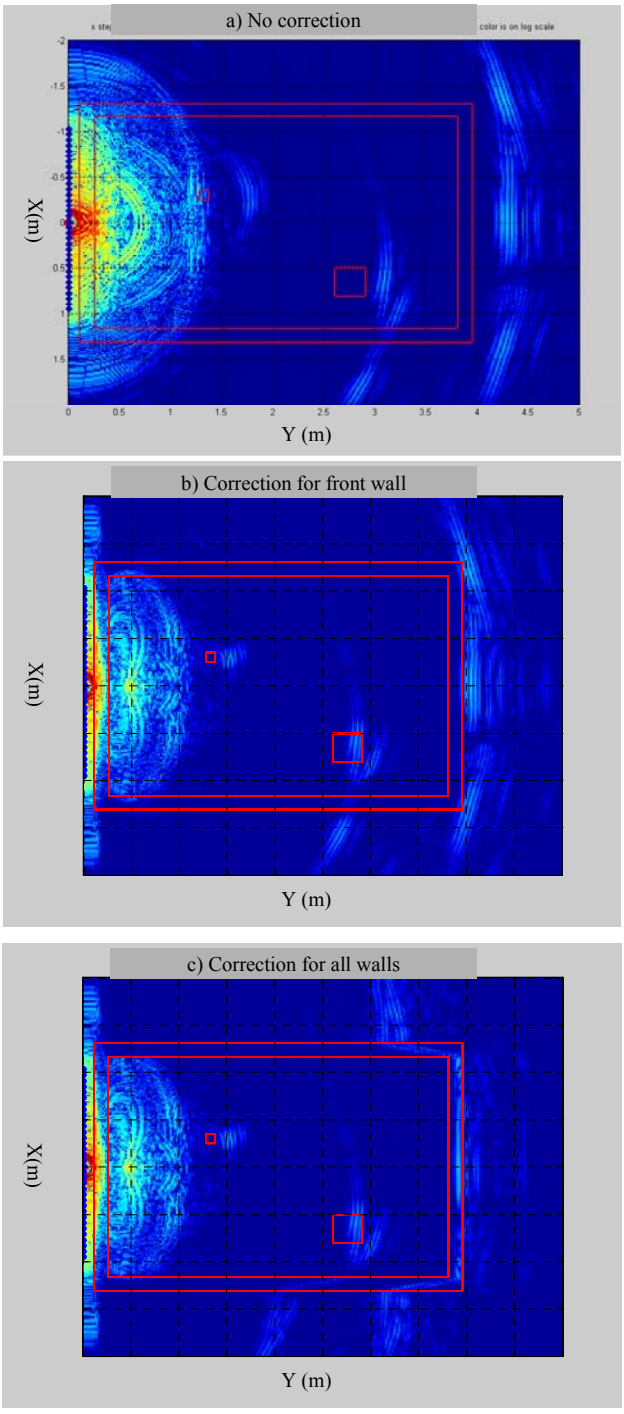

Figure 26. Static mapping a) without correction; b) correction for one wall; c) correction for four walls

6. Radar parameters and processing

This section examines the impact of various radar parameters on the resulting through wall radar images. The goal is to optimize the radar parameters and processing for the development of a future prototype or a radar test bed.

6.1 Sampling rate

The Nyquist theorem states that the sampling rate should be at least twice the signal frequency to avoid aliasing [17]. The signal that is transmitted by the UWB SP radar is shown in Figure 3. The center frequency is 2 GHz and the 3 dB upper frequency components is about 3 GHz [4]. Table 1 shows the sampling rate required for these frequencies to avoid aliasing.

Table 1. *Nyquist sampling rate*

SIGNAL PARAMETERS		NYQUIST RATE		
Frequency (GHz)	***Wavelength (cm)***	***Sampling rate (GS/s)***	***Time interval (s)***	***Range interval (cm)***
2	15	4	2.5e-10	7.5
3	10	6	1.67e-10	5

For the simulated data, each received signal or frame has 2000 bins and the interval time between each bin is 1.9258e-11 seconds (corresponding to 0.578 cm). The aliasing of the frequency component of 2 or 3 GHz can be avoided by taking every 8^{th} or 13^{th} bin of each frame respectively or less.

Table 2. *Simulated time bins parameters*

NUMBER OF BINS	TIME INTERVAL (10^{-10} S)	SAMPLING RATE (GS/S)	SAMPLING DISTANCE (CM)
1	0. 19258	51.93	0.578
6	1.1555	8.65	3.468
8	**1.5406**	**6.49**	**4.624**
9	1.7332	5.77	5.202
12	2.3110	4.33	6.936
13	**2.5035**	**3.99**	**7.514**
19	3.6590	2.73	10.982
25	4.8145	2.08	14.450

Figure 27 to 29 show the radar images of moving boxes using different sampling rates (or bin step) for the simulated received echoes. There is practically no difference using a bin step from one to eight, which represent a sampling rate of 51.9 and 6.5 GS/s respectively. The targets side lobes start to increase slowly from a bin step of 9 (5.6GS/s) and become considerable from bin step of 13 (4.0GS/s). These figures confirm the Nyquist theorem , which states that signals have to be sampled at twice their frequency to avoid aliasing. Sampling of at least twice the upper frequency of the spectrum provides the lowest side lobes for the targets.

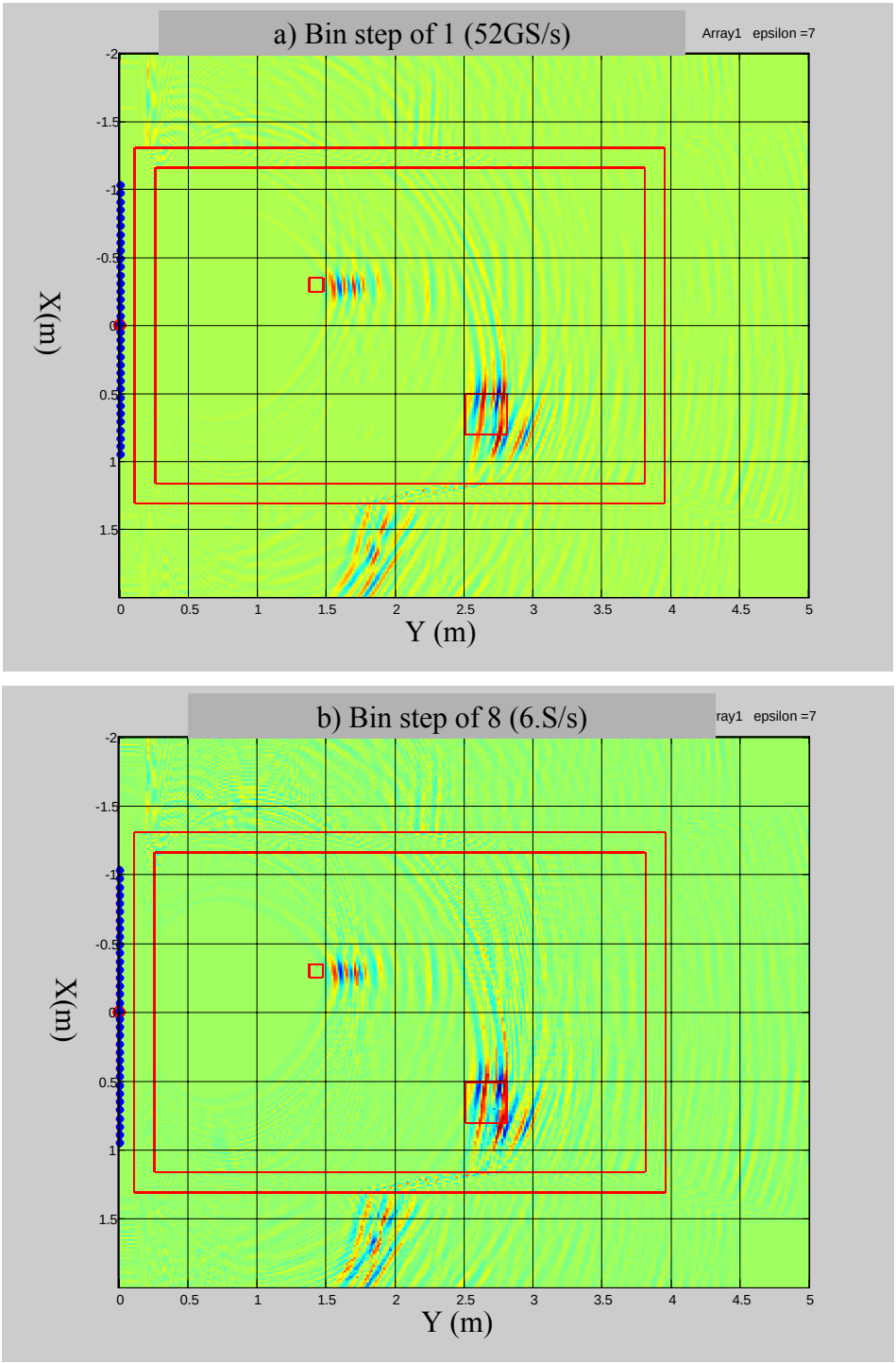

Figure 27. Bin step of 1 and 8 (sampling rate: 52 and 6.5GS/s)

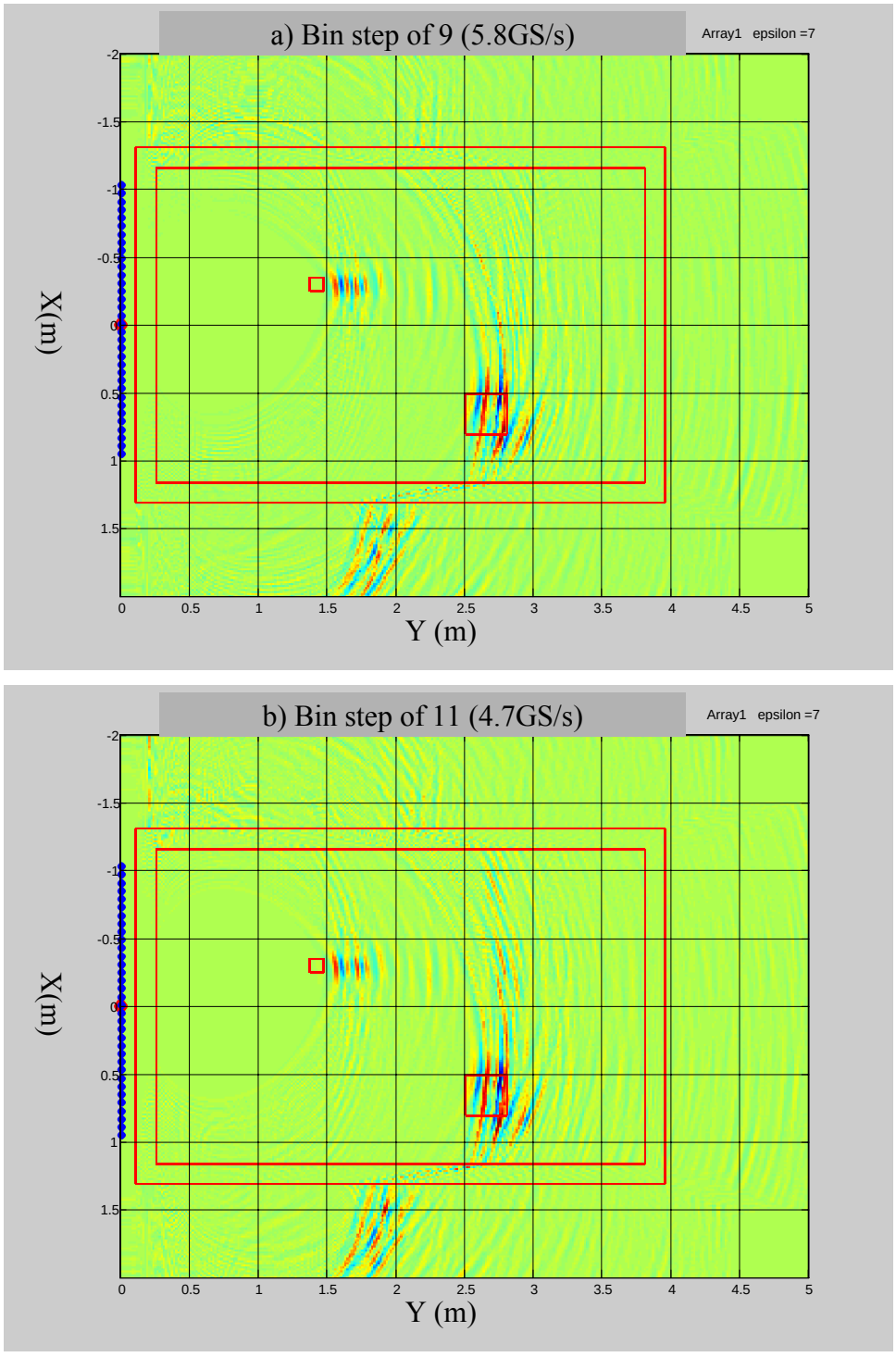

Figure 28.Bin step of 9 and 11 (sampling rate: 5.8 and 4.7GS/s)

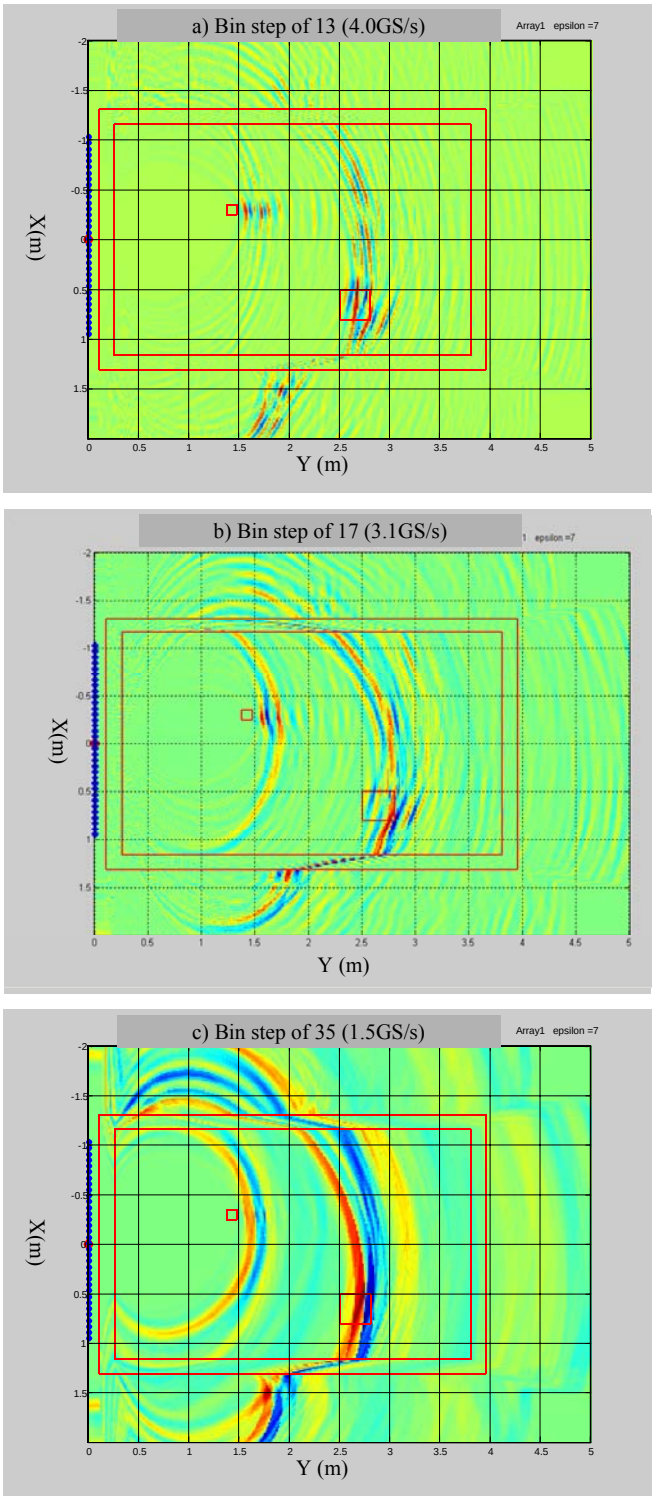

Figure 29.Bin step of 13, 17 and 35 (sampling rate of 4.0, 3.1 and 1.5GS/s)

6.2 Back projection pixel size

The back projection algorithm divides the whole image into a grid of small elements of surface or pixels. For each receiver, the amplitude of each time bin is recorded onto all possible grid elements based on the total flight time. This sub-section examines the impact of the pixel size on the resulting back projected radar images. Intuitively, the best pixel size should be the same as the radar range resolution. The range resolution is 7.5cm for this simulated radar data.

Figure 30 and 31 show radar images of both moving and stationary objects using pixel size from 1 to 10 cm. The smaller size of pixel produces smoother images of the targets and more details. For pixel sizes half the size of the radar range resolution, the targets images are more discontinuous. For pixel size the same size than the radar range resolution, radar image starts to be severely degraded. However, it should be noted that the spatial distribution of the target images stay in the same area but with more discontinuity. In summary, a pixel size smaller than the radar range resolution provides radar images of better quality. A pixel size that is seven times smaller than the radar range resolution is recommended.

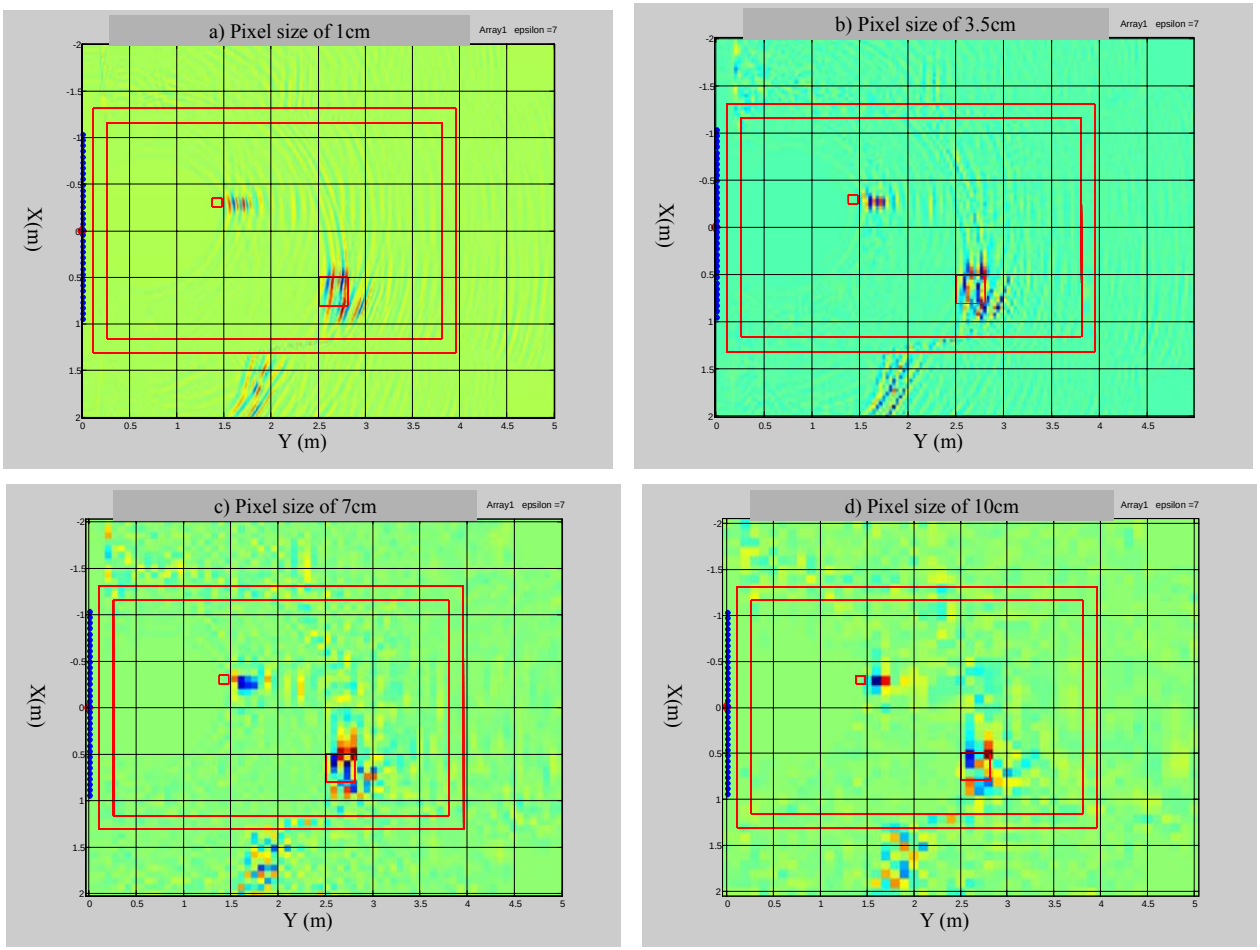

Figure 30. Moving targets: pixel size 1, 3.5, 7and 10cm

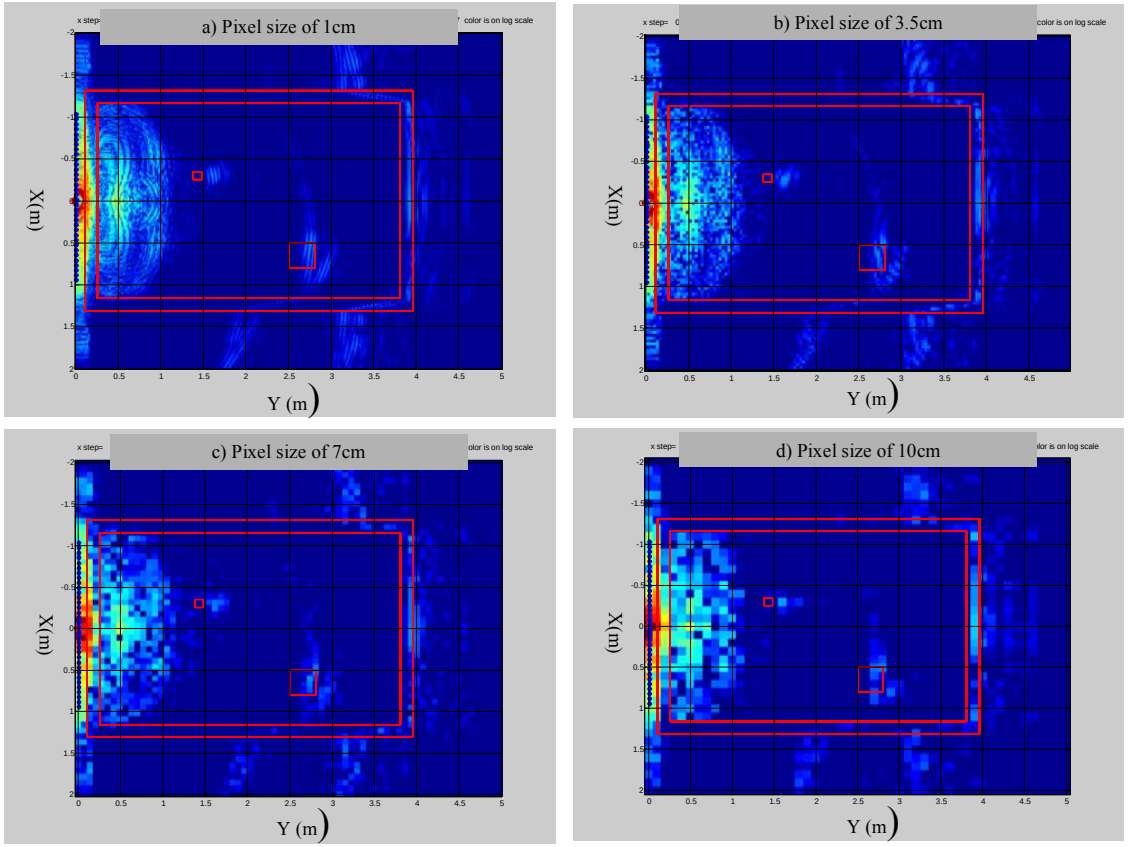

Figure 31 Static mapping: Pixel size 1, 3.5, 7and 10cm

6.3 Antenna parameters

6.3.1 Aperture size

In the simulation, the UWB SP signal is transmitted from a single antenna element and received by a receiving array. The beam width of the receiving array is a function of the transmitted wavelength and antenna aperture size as follows:

$$\theta = \frac{\lambda}{D} \tag{11}$$

where λ is the wavelength of the signal and D the aperture of the receiving antenna. If each antenna transmits and receives the signals, then the receiving array beam width is reduced by half. For the simulated data, the receiver cross range resolution at a given range R is given by:

$$\Delta R_c = \frac{\lambda}{D} R \tag{12}$$

The centre frequency of the simulated signal is 2 GHz, which corresponds to a wavelength of 15 cm. Figure 32 shows radar images of the moving boxes at position 5 using different sizes of receive antenna aperture. The cross range dimensions of the targets images correspond well to those predicted by Equation (12), and shown in the Table 3.

Table 3. *Cross range resolution*

	SMALL BOX		LARGE BOX	
Antenna aperture (m)	***Front box distance (m)***	***Cross range (cm)***	***Front box distance (m)***	***Cross range (cm)***
2.00	1.41	10.6	2.59	19.4
1.00	1.41	21.2	2.59	38.9
0.50	1.41	42.2	2.59	77.8
0.20	1.41	105.8	2.59	194.2

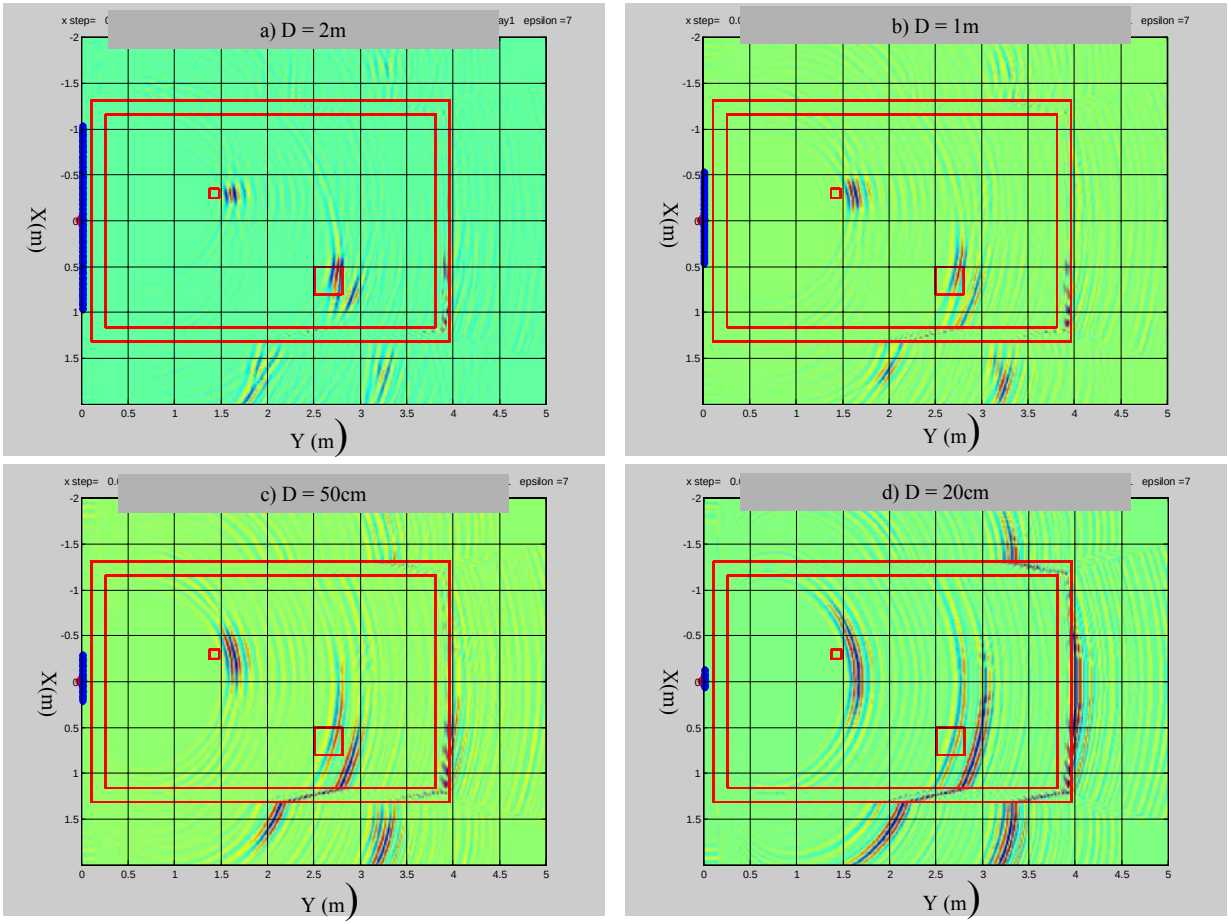

Figure 32. Antenna receiving aperture of 2m, 1m, 50cm and 20cm respectively.

6.3.2 Antenna spacing

This sub-section examines the impact of antenna spacing on the through wall radar images. This section examines whether the spacing between the antenna elements should be at least twice the centre frequency (every half wavelength) as stated by the Nyquist theorem. For 2 GHz, the centre frequency, the antenna spacing should be less than 7.5 cm to avoid aliasing. For 3GHz, the upper frequency components, the antenna spacing should be less than 5 cm.

Figure 33 shows radar images obtained with the same antenna aperture size but with antennas spacing of 2, 6, 8 and 10 cm respectively. The cross range resolution of the targets does not change with antenna spacing, as expected from equation 11. There are no major differences in the radar images obtained using antenna spacing of 2 and 6 cm. Radar images obtained using antenna spacing of 8 and 10 cm produce very similar target images but the side lobes start to rise. Once again, this confirms the Nyquist theorem that sampling rate should be twice the sampled frequency to avoid aliasing. Figure 34 shows radar images obtained with the same antenna aperture but with antenna spacing of 14, 26, 36, and 50 cm respectively. Target side lobes become stronger and are closer to the main beam (or targets position) when the antenna spacing is increased. In summary, the beam width of the receiving array is a function of its aperture size. The side lobes are a function of the antenna element spacing.

Figure 35 shows radar images obtained using an antenna array having 5 antenna elements in the first case and one additional antenna element in the second case. The sixth element is closest to the large box. A larger antenna aperture should produce better radar images but in this case this is not true. In fact, the target side lobes of the large box are increased considerably when the sixth antenna element is added. In fact, the antenna element being closest to the large box receives an echo much stronger than other receiving elements. As a result, its amplitude contribution is not well cancelled by the contribution from the other antenna elements. The benefit of a larger antenna size, in this case, does not show up when the resulting target image is dominated by one antenna element.

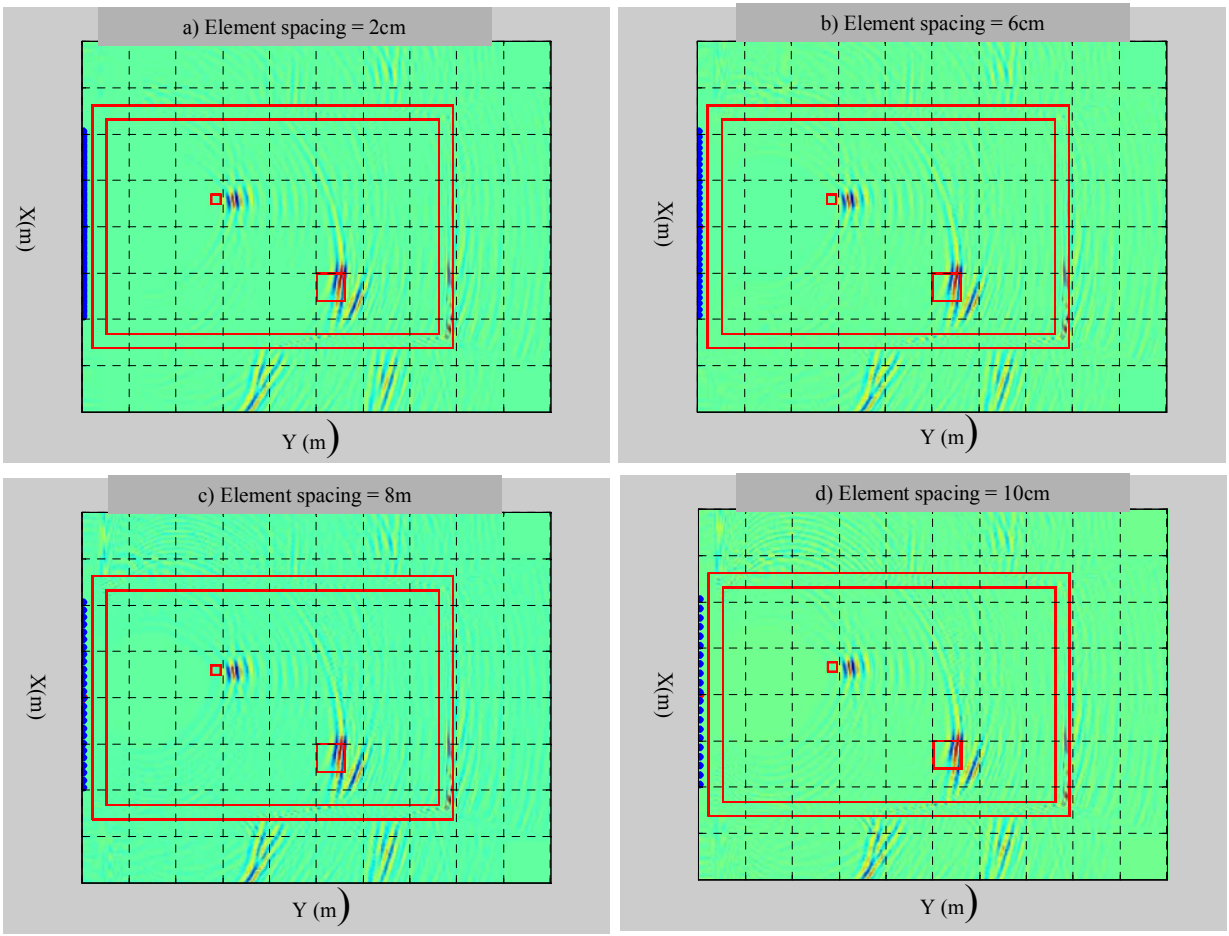

Figure 33. 2m antenna receiving aperture with element spacing of 2cm, 6cm, 8cm and 10cm.

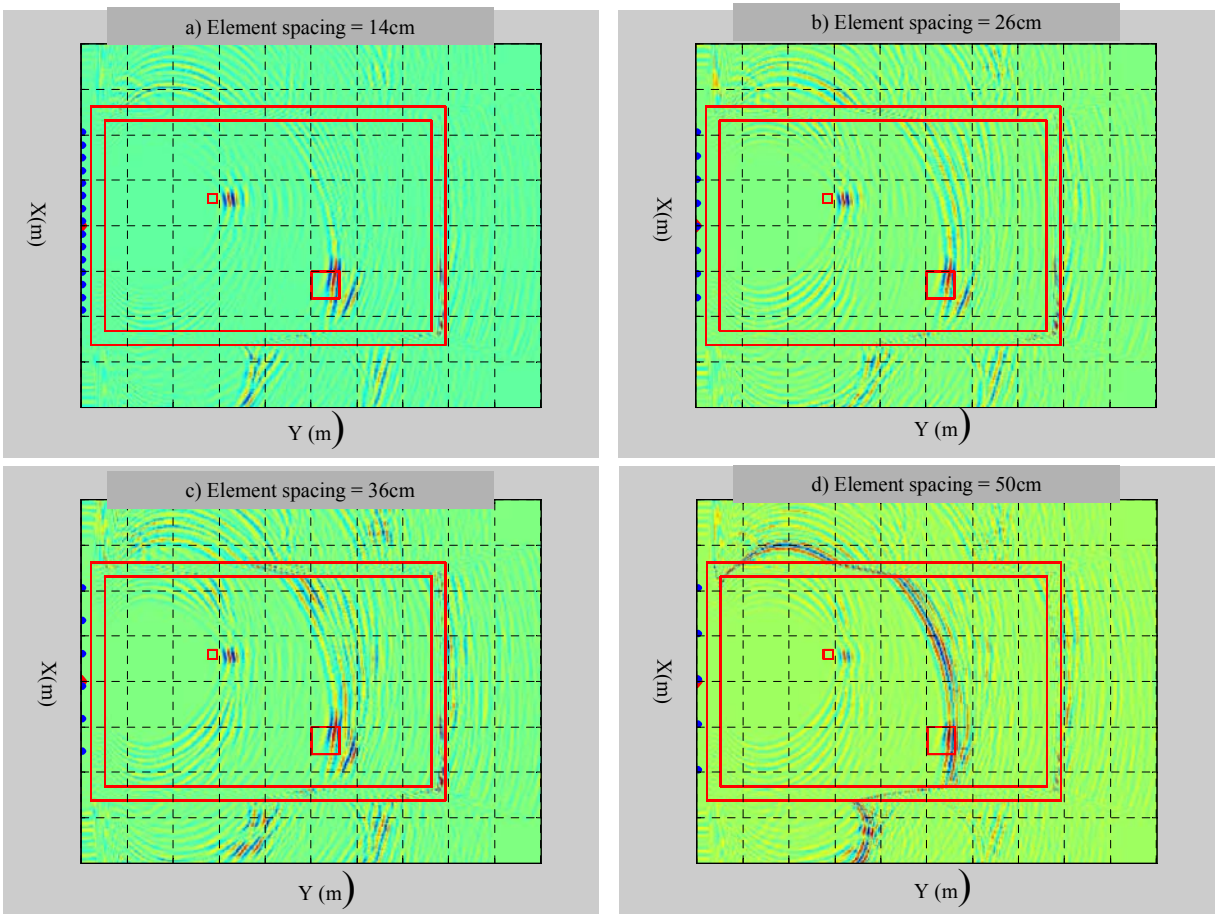

Figure 34. 2m antenna aperture with element spacing of 14, 26, 36 and 50cm

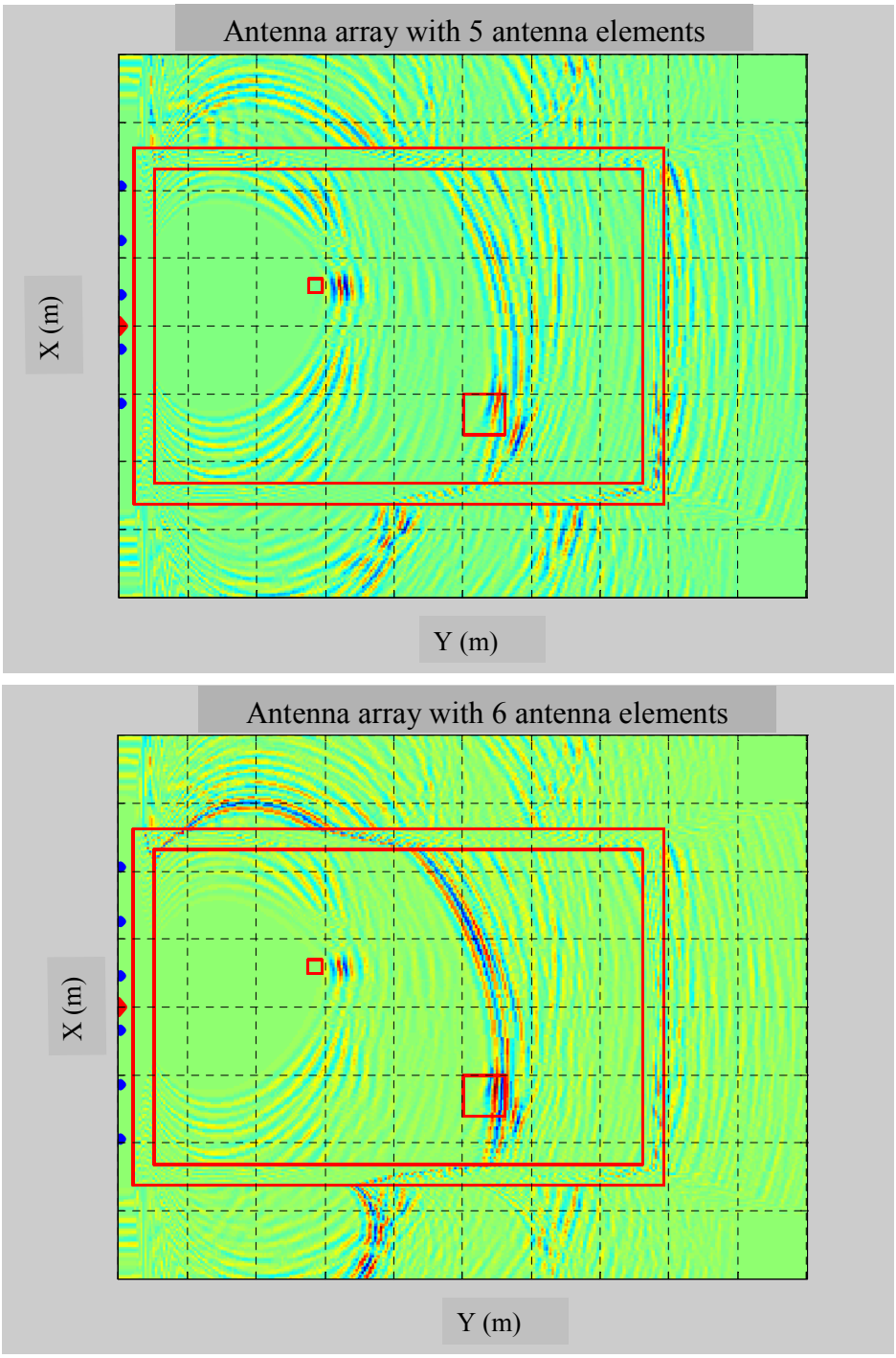

Figure 35. Antenna arrays having 6 and 5 antennas elements respectively

7. Multistatic through wall radar surveillance

This section examines the capability of multistatic UWB SP radar to provide through-wall surveillance. The back projection algorithm records the amplitude of each received time bin on a spatial grid at each pixel where the signal can come from based on the total flight time. The region of constant time of flight is circular when the transmitting and receiving antennas are collocated. Otherwise this region is parabolic as shown in Figure 36. The presence of the walls will change the region of constant flight time as shown in Figure 37.

7.1 No walls cases

The best way to demonstrate the capability of UWB SP multistatic radar to provide through wall surveillance is first to examine the capabilities without the presence of the walls.

Figure 38, Figure 39 and Figure 40 shows radar images of both moving targets and static mapping without the presence of concrete walls. The images have been obtained with the same receiver array but at different positions along the front, side and back walls. These positions correspond to a sub-array of arrays 1, 4 and 2 of Figure 1. On Figure 38, the moving targets are clearly visible and localized on the radar images obtained using sub-array 1 (front wall). In Figure 39 the moving targets obtained using sub-array 4 (sidewall) look good in one case and considerably spread in space in the other. On Figure 40, the moving targets obtained using sub-array 2 (back wall) are very spread in space for both cases.

A close inspection of the corresponding radar images with static mapping show that the direct signal is spread along a parabolic curve and is very strong. If the boxes are located within that region then the radar images of the moving boxes will be very spread in space due to the parabolic curve. For moving targets the clutter suppression technique does not work as well since the direct coupling is different from the frame-to-frame or the empty room response. As a result, the frame-to-frame subtraction will still include a strong contribution from the direct signal. UWB SP multistatic radar works relatively well as long as the targets are not located in the direct coupling region, i.e., as long as the indirect echoes arrive after the direct signal.

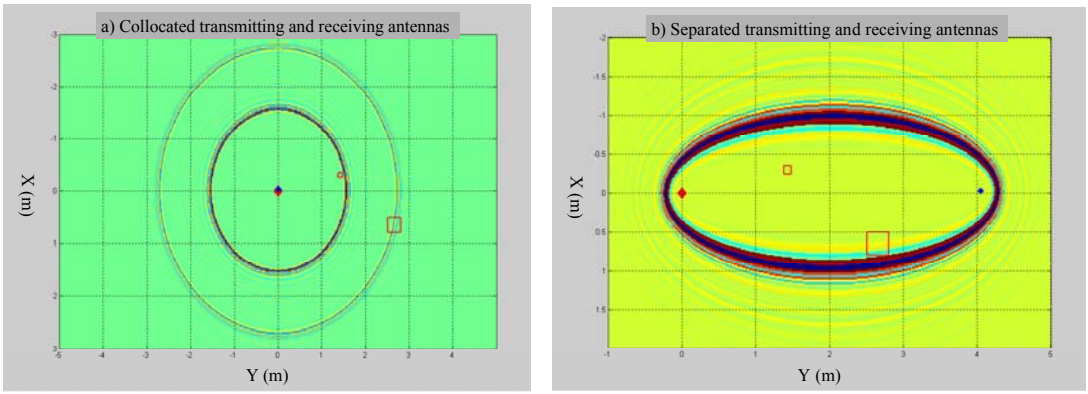

Figure 36. No room case with transmitting and receiving antennas: a) collocated; b) separated

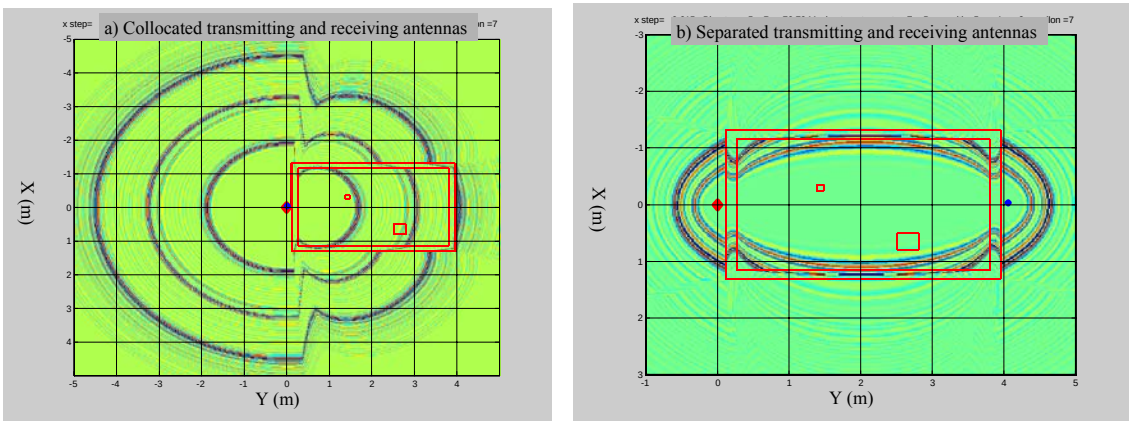

Figure 37. Concrete room with transmitting and receiving antennas: a) collocated; b) separated

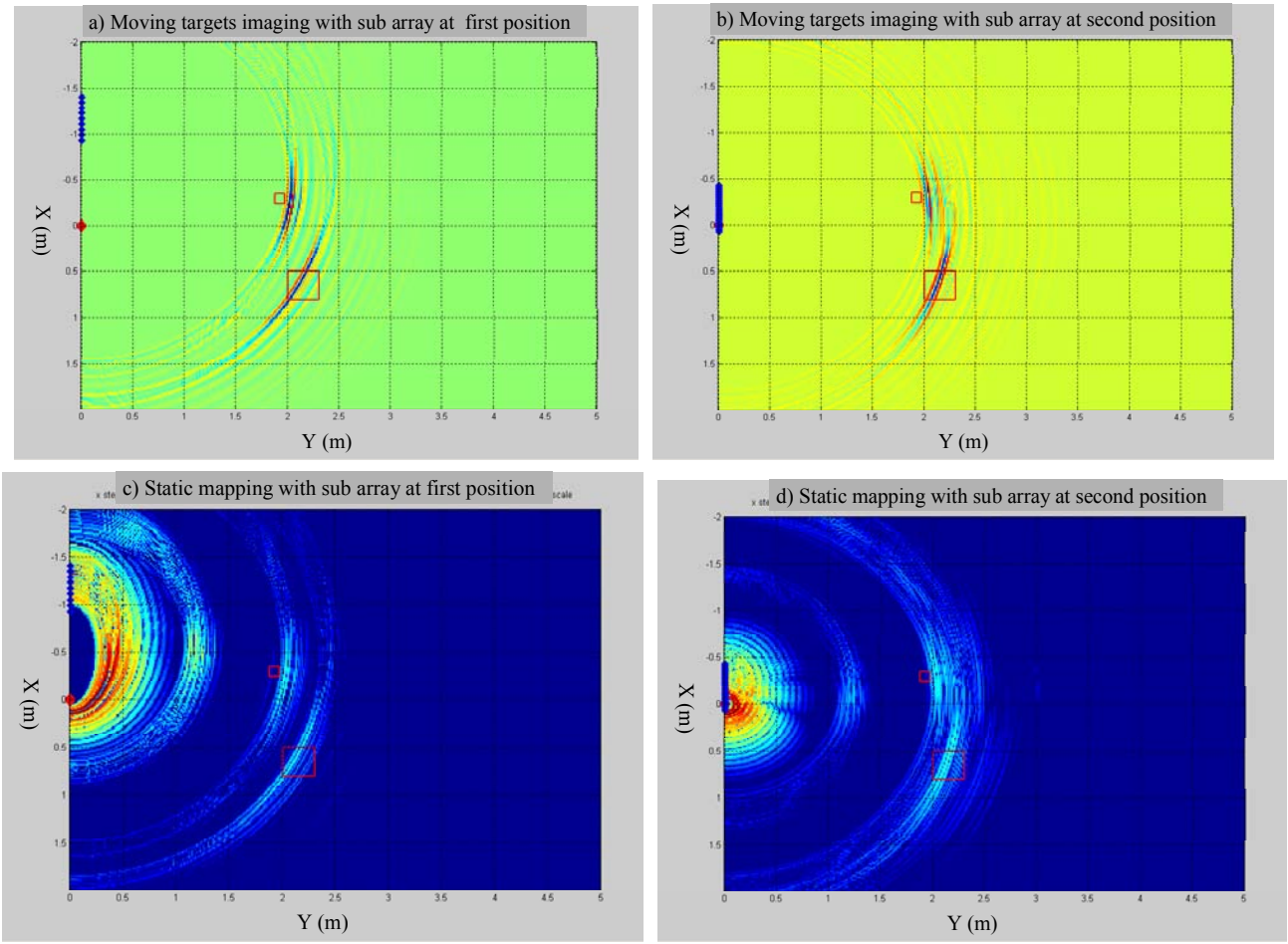

Figure 38. Radar images of moving targets and fixed objects without walls for two receiving array position along front wall

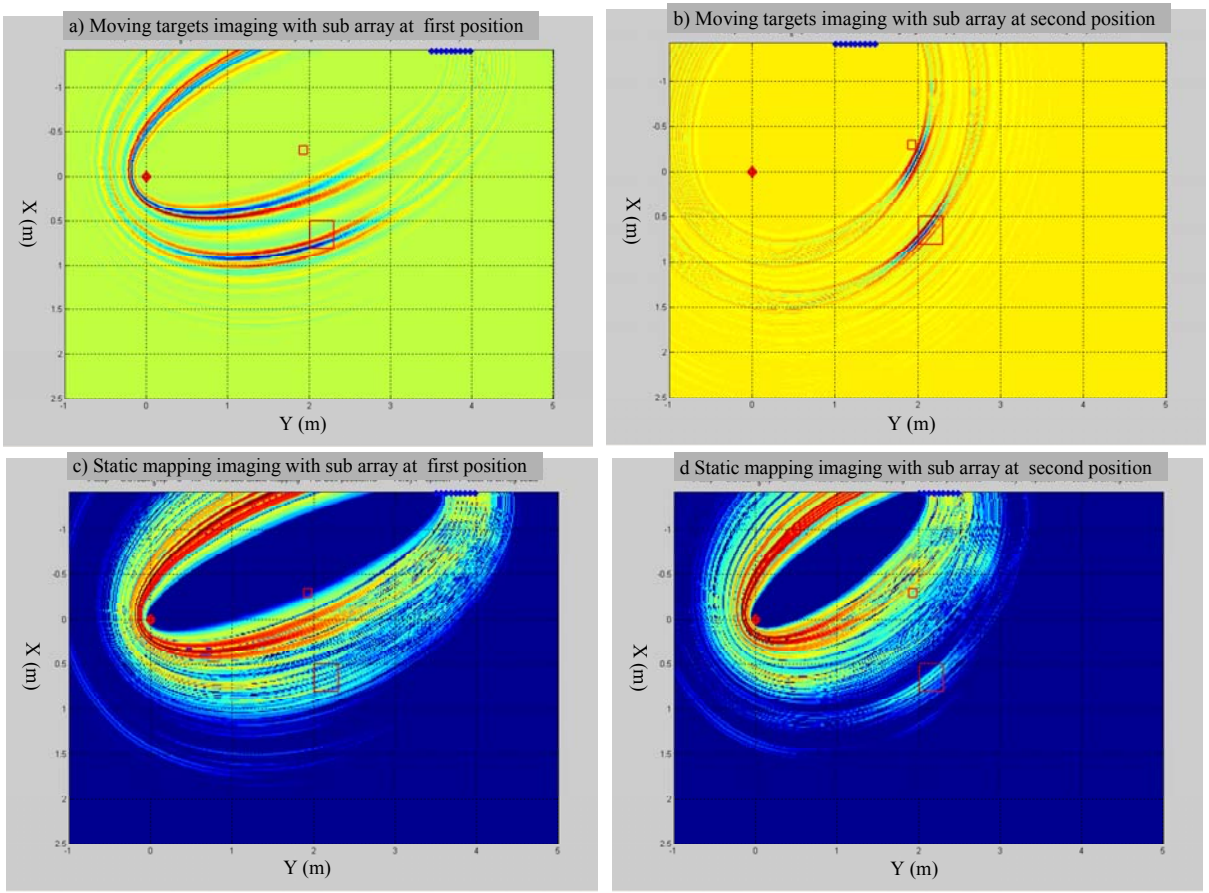

Figure 39. Radar images of moving targets and fixed objects without walls for two receiving array position along sidewall

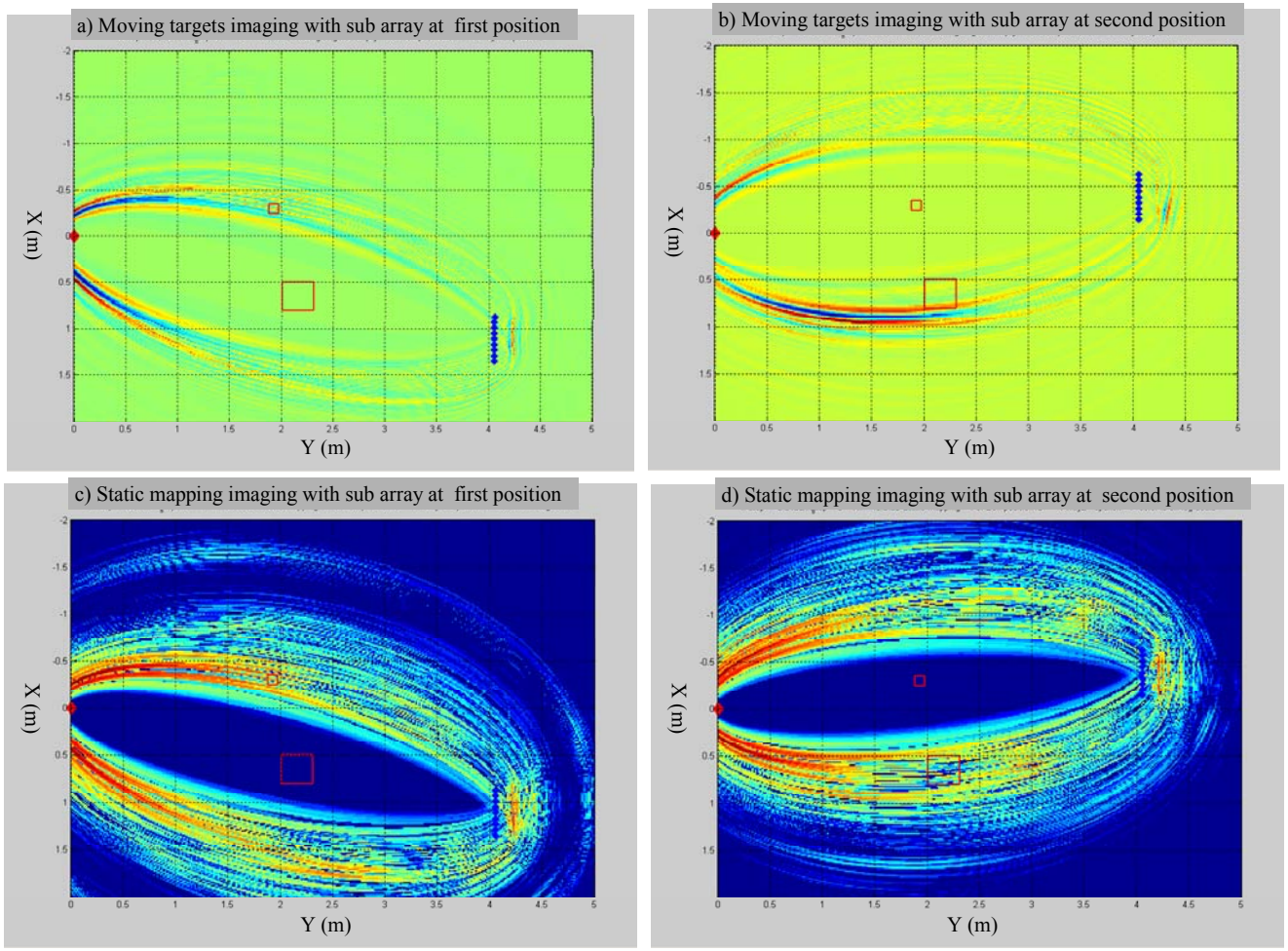

Figure 40. Radar images of moving targets and fixed objects without walls for two receiving array position along back wall

7.2 Concrete room

Figure 41 shows radar images of "moving boxes" obtained with a receiving array located along one of the side walls but inside the concrete room. As in the previous sub-section, the targets images are well localized in one case and very spread in space in the other. Figure 42 shows the same images, but with static mapping. Once again, if the target is outside the direct coupling region then the targets images are well localized in space. Figure 43 shows radar images of moving targets obtained with a receiving array located along the back wall inside the concrete room. Of interest, there are target images outside the room that move with the boxes. In fact, the transmitted signals are reflected back by the boxes and rebounds on the front wall. As a result, the receiver array is producing target images of these front wall reflections.

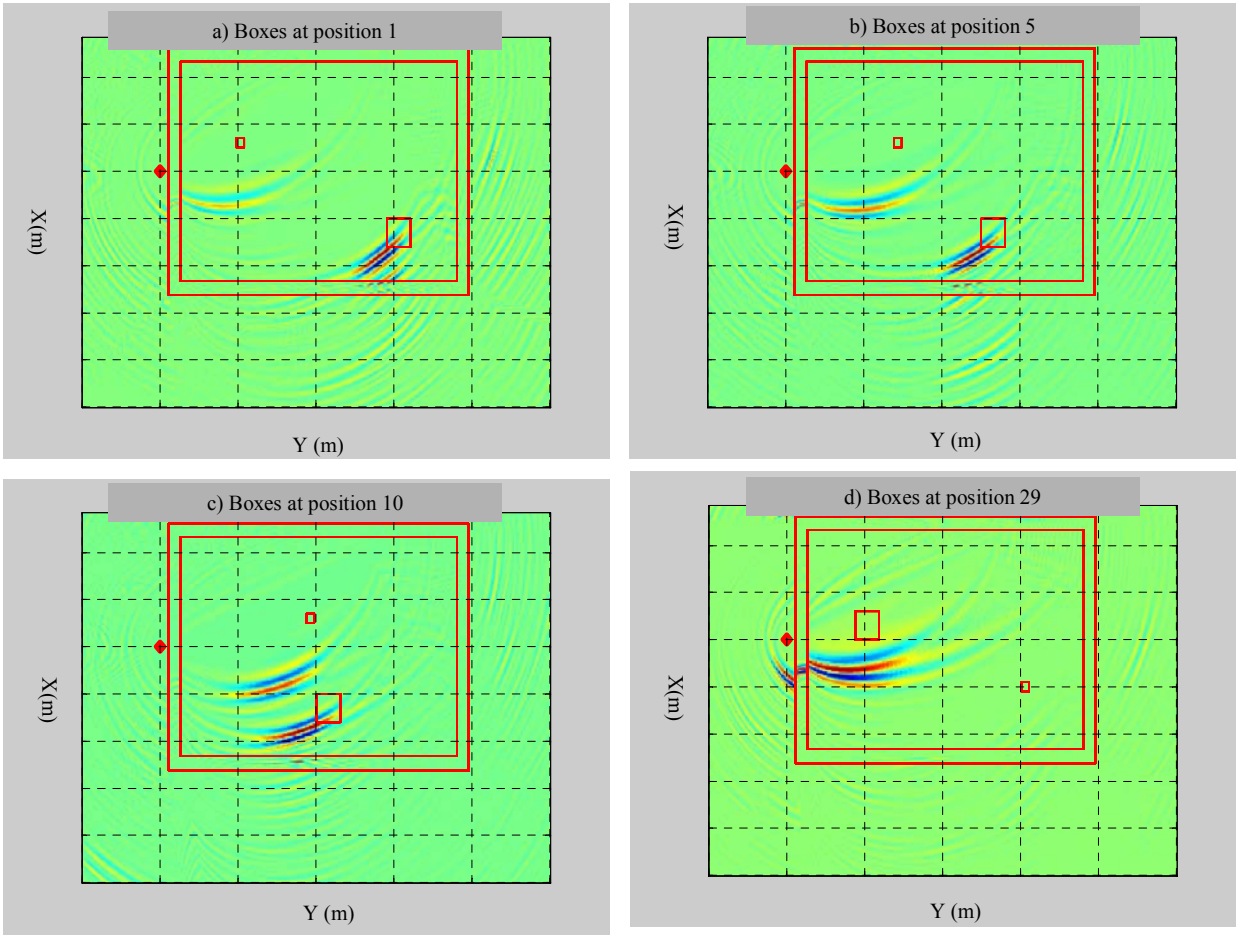

Figure 41. Radar images of moving targets including concrete room with receiving array along sidewall

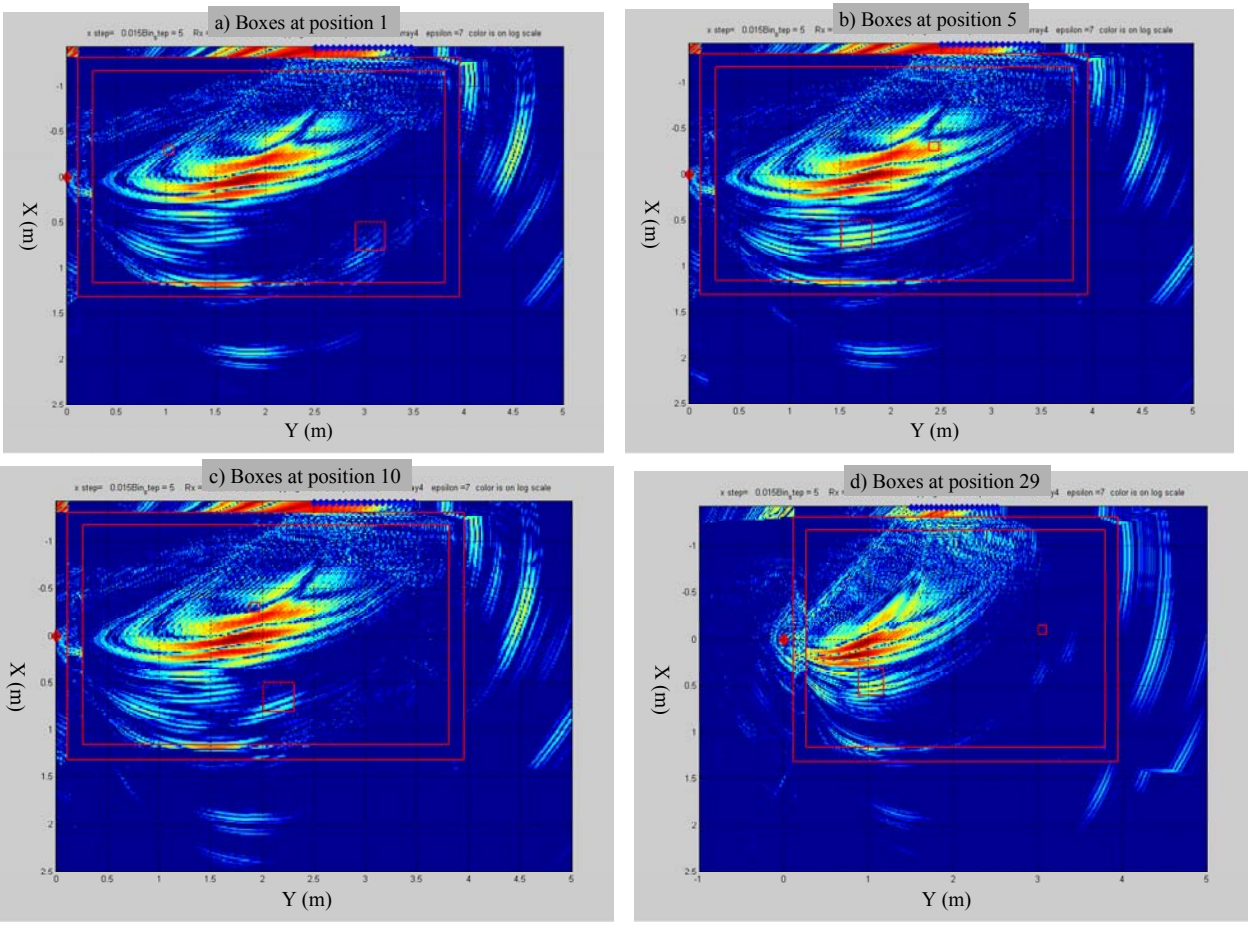

Figure 42. Radar images of fixed objects including concrete room with receiving array along sidewall

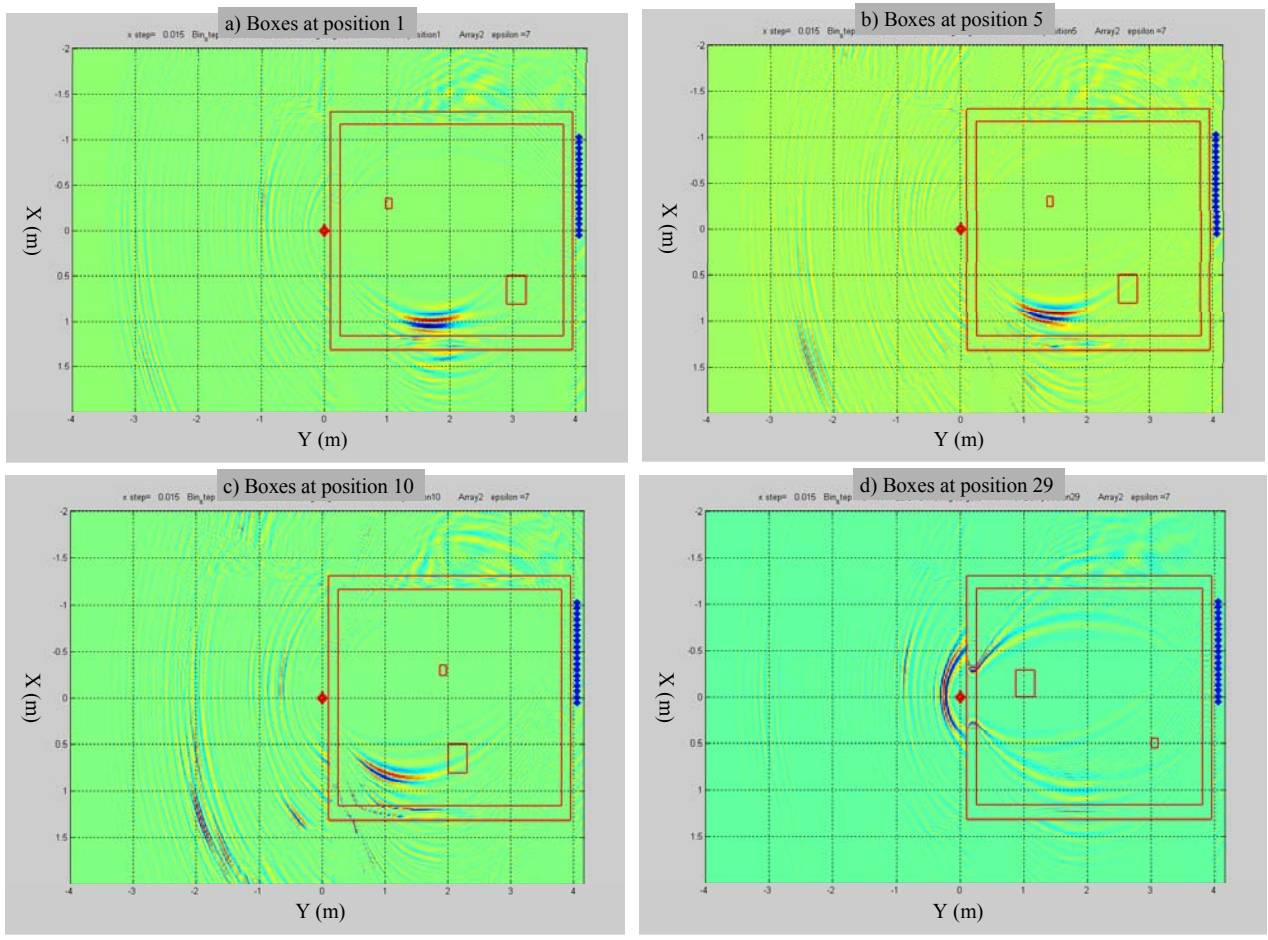

Figure 43. Radar images of moving targets including concrete room with receiving array along back wall

8. Conclusion

This report has shown that UWB SP radar can provide surveillance through concrete walls.

The simulated data shows that electromagnetic (EM) wave can propagate into the concrete room and excite the targets inside the room. The presence of walls or targets is clearly visible in the received signal.

The radar images show that UWB SP radar can track the targets moving inside the concrete room or can produce static mapping of the room layout including desired targets. This is important since buildings with concrete walls or brick walls are very common throughout the world and is the most likely type of building to be encountered by the Canadian Forces during military operations in urban areas.

Concrete walls have several effects on through-wall imaging. They defocuse target images and displace them from their true position. False targets can also be present on the radar images. The radar images clearly show that velocity correction considerably improves the focusing and quality of the radar images.

In static mapping, the amplitude of the signal received directly from the transmitting antenna is much larger that the echoes received from stationary objects. A logarithmic color scale has to be used to show both the strong and the weaker echoes from the targets.

UWB SP radar can also be used to conduct multistatic through-wall surveillance. Multistatic through wall imaging works well as long as the targets are not located in the direct coupling region, i.e., as long as the indirect echoes arrive after the direct signal.

9. References

1. Tunaley, J., (March 2001), *Evaluation of Ka-Band Homodyne Radar for Short Range Surveillance and Target Classification*, Contract W7714-0357 for DREO, 70 pages

2. Tunaley, J., (March 2002), *Through-the-wall UWB Processing*, Contract W7714-1-0558 for DRDC Ottawa, 100 pages

3. Gauthier, S.M. and Chamma, W., (2002), *Through-The-Wall Surveillance*, DRDC Ottawa TM 2002-108

4. Chamma, W. and Kashyap, S., (2003), *Detection of Targets Behind Walls Using Ultra Wideband Short Pulse*, Ultra-wideband Short-pulse Electromagnetics 6, E. Mokole et al., Plenum Press

5. Hung, E, and Gauthier, S., (2002), *The Beam Patterns of UWB Radars with Uniform Linear Tx and Rx Antenna Arrays*, DRDC Ottawa TM 2002-168

6. Foo, S., (2002), *EM Modeling of UWB Through-Wall Radar Imaging Using The High-Frequency Geometrical Optics (GO)*, DRDC Ottawa TM 2002-166

7. (2002), *Through-wall X-band Experiments*, Comlab Inc under contract W7714-010582/001/SV,

8. Gauthier, S., Chamma, W., et al, (Dec 2002), *Through-The-Wall Surveillance*, 5th International Military Sensing Symposium, Washington, Dec 2002

9. Barrie, G., (2003) *Ultra-wideband Synthetic Aperture: Data and Image Processing*, DRDC Ottawa TM 2003-015

10. Hung, E, Chamma, W. and Gauthier, S., (2003), *UWB Receive Array Beamformer Output Images of Objects in a Concrete Room*, DRDC Ottawa TN 2003-062

11. Robinson, R, (2003), *Through the wall ultra wideband radar*, Contract Document, DRDC Ottawa CR 2003-023

12. (2003), *Ultra-Wideband Radar Through-Wall Measurements*, Comlab Inc under contract W7714-020650/001/SV,

13. Hung, E, Chamma, W. and Gauthier, S., (2003), *A second Study of UWB Receive Array Beamformer Output Images of Objects in a Room*, DRDC Ottawa TM 2003-nnn

14. Leblanc, L.J. and Tondreau, J.R., (2003), *Surveillance Requirements for Military Operations in Urban Terrain*, Land Force Technical And Staff report, June 2003

15. Lorrain, P. and Corson, D., (1970), *Electromagnetic Fields and Waves*, W.H. Freeman and Company

16. Skolnik, M.L., (1980), Introduction to Radar Systems, McGraw-Hill Book Company

17. Oppenheim, A.V. and Willsky, A.S., (1997), *Signals & Systems Second Edition*, Prentice Hall Signal Processing Series

Annex A: Boxes position coordinates

Table 4. *Boxes coordinates for each position number*

	SMALL BOX		LARGE BOX	
Position	***X centre (m)***	***Y centre (m)***	***X centre (m)***	***Y Centre (m)***
1	-0.30	1.03	0.65	3.06
2	-0.30	1.13	0.65	2.96
3	-0.30	1.23	0.65	2.86
4	-0.30	1.33	0.65	2.76
5	-0.30	1.43	0.65	2.66
6	-0.30	1.53	0.65	2.56
7	-0.30	1.63	0.65	2.46
8	-0.30	1.73	0.65	2.36
9	-0.30	1.83	0.65	2.26
10	-0.30	1.93	0.65	2.16
11	-0.30	2.03	0.65	2.06
12	-0.30	2.13	0.65	1.96
13	-0.30	2.23	0.65	1.86
14	-0.30	2.33	0.65	1.76
15	-0.30	2.43	0.65	1.66
16	-0.30	2.53	0.65	1.56
17	-0.30	2.63	0.65	1.46
18	-0.30	2.73	0.65	1.36
19	-0.30	2.83	0.65	1.26
20	-0.30	2.93	0.65	1.16
21	-0.30	3.06	0.65	1.03
22	-0.20	3.06	0.55	1.03
23	0.10	3.06	0.45	1.03
24	000	3.06	0.35	1.03
25	0.10	3.06	0.25	1.03
26	0.20	3.06	0.15	1.03
27	0.30	3.06	0.05	1.03
28	0.40	3.06	-0.05	1.03
29	0.50	3.06	-0.15	1.03
30	0.65	3.06	-0.30	1.03

Annex B: Antenna elements coordinates

Figure 1 shows the position of the transmitting element and all receiving antennas elements. The transmitter (Tx) consists of 1 antenna element located at (0, 0, 100cm). The receiver (Rx) elements on each Rx Array are spaced by 2.0cm along their direction. The coordinates of all antenna elements are given in Table 5 to 9.

Table 5. *Transmitter (1 element)*

Element #	***X (cm)***	***Y (cm)***	***Z (cm)***
1	0	0	10

Table 6. *Rx Array 1 (142 elements)*

Element #	***X (cm)***	***Y (cm)***	***Z (cm)***
1	-141	1	100
2	-139	1	100
3	-137	1	100
…	…	…	…
140	+137	1	100
141	+139	1	100
142	+141	1	100

Table 7. *Rx Array 2 (142 elements)*

Element #	***X (cm)***	***Y (cm)***	***Z (cm)***
1	-141	406	100
2	-139	406	100
3	-137	406	100
…	…	…	…
140	+137	406	100
141	+139	406	100
142	+141	406	100

Table 8. *Rx Array 3 (203 elements)*

Element #	***X (cm)***	***Y (cm)***	***Z (cm)***
1	+141	3	100
2	+141	5	100
3	+141	7	100
…	…	…	…
140	+141	401	100
141	+141	403	100
142	+141	405	100

Table 9. *Rx Array 4 (203 elements)*

Element #	***X (cm)***	***Y (cm)***	***Z (cm)***
1	-141	3	100
2	-141	5	100
3	-141	7	100
…	…	…	…
140	-141	401	100
141	-141	403	100
142	-141	405	100

List of symbols/abbreviations/acronyms/initialisms

DND	Department of National Defence
CF	Canadian Forces
MTI	Moving Target Indicator
UWB	Ultra-wideband
SP	Short-pulse

DOCUMENT CONTROL DATA

(Security classification of title, body of abstract and indexing annotation must be entered when the overall document is classified)

1. ORIGINATOR (the name and address of the organization preparing the document. Organizations for whom the document was prepared, e.g. Establishment sponsoring a contractor's report, or tasking agency, are entered in section 8.)

Defence R&D Canada – Ottawa
Ottawa ON
K1A 0Z4

2. SECURITY CLASSIFICATION (overall security classification of the document, including special warning terms if applicable)

UNCLASSIFIED

3. TITLE (the complete document title as indicated on the title page. Its classification should be indicated by the appropriate abbreviation (S,C or U) in parentheses after the title.)

Surveillance Through Concrete Walls (U)

4. AUTHORS (Last name, first name, middle initial)

Gauthier Sylvain; M.Hung, Eric K.L.; Chamma, Walid

5. DATE OF PUBLICATION (month and year of publication of document)	6a. NO. OF PAGES (total containing information. Include Annexes, Appendices, etc.)	6b. NO. OF REFS (total cited in document)
December 2003	81	16

7. DESCRIPTIVE NOTES (the category of the document, e.g. technical report, technical note or memorandum. If appropriate, enter the type of report, e.g. interim, progress, summary, annual or final. Give the inclusive dates when a specific reporting period is covered.)

Technical memorandum

8. SPONSORING ACTIVITY (the name of the department project office or laboratory sponsoring the research and development. Include the address.)

DRDC Ottawa

9a. PROJECT OR GRANT NO. (if appropriate, the applicable research and development project or grant number under which the document was written. Please specify whether project or grant)	9b. CONTRACT NO. (if appropriate, the applicable number under which the document was written)
12kc15	

10a. ORIGINATOR'S DOCUMENT NUMBER (the official document number by which the document is identified by the originating activity. This number must be unique to this document.)	10b. OTHER DOCUMENT NOS. (Any other numbers which may be assigned this document either by the originator or by the sponsor)
DRDC Ottawa TM 2003-233	

11. DOCUMENT AVAILABILITY (any limitations on further dissemination of the document, other than those imposed by security classification)

(x) Unlimited distribution
( ) Distribution limited to defence departments and defence contractors; further distribution only as approved
( ) Distribution limited to defence departments and Canadian defence contractors; further distribution only as approved
( ) Distribution limited to government departments and agencies; further distribution only as approved
( ) Distribution limited to defence departments; further distribution only as approved
( ) Other (please specify):

12. DOCUMENT ANNOUNCEMENT (any limitation to the bibliographic announcement of this document. This will normally correspond to the Document Availability (11). However, where further distribution (beyond the audience specified in 11) is possible, a wider announcement audience may be selected.)

Unlimited

13. ABSTRACT (a brief and factual summary of the document. It may also appear elsewhere in the body of the document itself. It is highly desirable that the abstract of classified documents be unclassified. Each paragraph of the abstract shall begin with an indication of the security classification of the information in the paragraph (unless the document itself is unclassified) represented as (S), (C), or (U). It is not necessary to include here abstracts in both official languages unless the text is bilingual).

This report studies the capability of ultra wideband short-pulse (UWB SP) radar to provide through concrete walls surveillance including multistatic radar surveillance. Multistatic radar configurations are of interest since they can be used to do covert surveillance.

A full wave electromagnetic simulator is used to generate high fidelity through wall radar data. These raw radar data are transformed into radar images using a generation image algorithm that is described in detail in this report. The delay of the electromagnetic wave due to concrete walls when included into the imaging algorithm considerably improves the radar images. The impact of various radar parameters and signal processing techniques on radar images are examined in detail. The goal is to optimize the development of a potential radar testbed for through-wall imaging applications.

Radar images obtained using the image generation algorithm show that UWB SP radar can track targets moving inside a concrete room. The decrease in signal velocity within concrete walls has three effects on through-the-wall-imaging. It defocuses target images and displaces targets from their true positions. False targets can also be present in the radar images.

The radar images are considerably improved by including the time of flight difference due to concrete walls into the image generation algorithm. Radar images of stationary objects, or the room layout, obtained using the image generation algorithm show that UWB SP radar can provide static mapping of the concrete room layout. Radar images obtained using different multistatic radar configurations show that multistatic imaging works as long as targets are not located in the direct coupling region.

14. KEYWORDS, DESCRIPTORS or IDENTIFIERS (technically meaningful terms or short phrases that characterize a document and could be helpful in cataloguing the document. They should be selected so that no security classification is required. Identifiers such as equipment model designation, trade name, military project code name, geographic location may also be included. If possible keywords should be selected from a published thesaurus. e.g. Thesaurus of Engineering and Scientific Terms (TEST) and that thesaurus-identified. If it is not possible to select indexing terms which are Unclassified, the classification of each should be indicated as with the title.)

Ultra-wideband (UWB)
Short-pulse (SP) Radars
Rx array location
Concrete walls
Peak image power
Range dependence
Through the wall surveillance

Defence R&D Canada

Canada's leader in defence
and national security R&D

R & D pour la défense Canada

Chef de file au Canada en R & D
pour la défense et la sécurité nationale

www.drdc-rddc.gc.ca